

AD-A143 393

EXPERIMENTS IN OBJECTIVE AVIATION WEATHER FORECASTING
USING UPPER-LEVEL STEERING(U) AIR FORCE GEOPHYSICS LAB
HANSCOM AFB MA H S MUENCH 13 DEC 83 AFGL-TR-83-0328

1/1

UNCLASSIFIED

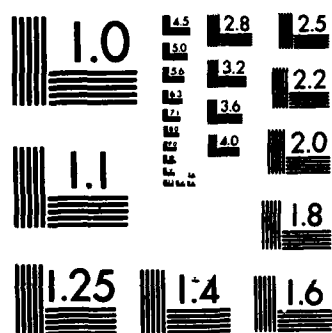
F/G 4/2

NL

END

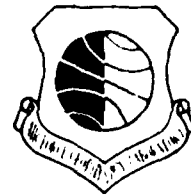
FILED

DTM



MICROCOPY RESOLUTION TEST CHART
NATIONAL BUREAU OF STANDARDS-1963-A

AFGL-TR-83-0328
ENVIRONMENTAL RESEARCH PAPERS, NO. 983



12

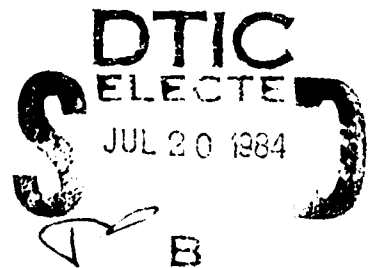
Experiments in Objective Aviation Weather Forecasting Using Upper-Level Steering

H. STUART MUENCH

AD-A143 393

13 DECEMBER 1983

Approved for public release; distribution unlimited.



ATMOSPHERIC SCIENCES DIVISION PROJECT 6670
AIR FORCE GEOPHYSICS LABORATORY
HANSCOM AFB, MASSACHUSETTS 01731

AIR FORCE SYSTEMS COMMAND, USAF




DTIC FILE COPY


84 07 19 006

This report has been reviewed by the ESD Public Affairs Office (PA) and is releasable to the National Technical Information Service (NTIS).

"This technical report has been reviewed and is approved for publication"

FOR THE COMMANDER


DONALD A. CHISHOLM, Chief
Atmospheric Prediction Branch


ROBERT A. McCLATCHEY, Director
Atmospheric Sciences Division

Qualified requestors may obtain additional copies from the Defense Technical Information Center. All others should apply to the National Technical Information Service.

If your address has changed, or if you wish to be removed from the mailing list, or if the addressee is no longer employed by your organization, please notify AFGL/AA, Hanscom AFB, MA 01731. This will assist us in maintaining a current mailing list.

Do not return copies of this report unless contractual obligations or notices on a specific document requires that it be returned.

Unclassified

SECURITY CLASSIFICATION OF THIS PAGE (When Data Entered)

REPORT DOCUMENTATION PAGE		READ INSTRUCTIONS BEFORE COMPLETING FORM
1. REPORT NUMBER AFGL-TR-83-0328	2. GOVT ACCESSION NO. A143393	3. CONTRACTOR'S CATALOG NUMBER
4. TITLE (and Subtitle) EXPERIMENTS IN OBJECTIVE AVIATION WEATHER FORECASTING USING UPPER- LEVEL STEERING		5. TYPE OF REPORT & PERIOD COVERED Final 1 Oct 81 - 30 Sep 83
7. AUTHOR(s) H. Stuart Muench		6. PERFORMING ORG. REPORT NUMBER ERP No. 863
9. PERFORMING ORGANIZATION NAME AND ADDRESS Air Force Geophysics Laboratory (LYP) Hanscom Air Force Base Massachusetts 01731		8. CONTRACT OR GRANT NUMBER(s)
11. CONTROLLING OFFICE NAME AND ADDRESS Air Force Geophysics Laboratory (LYP) Hanscom Air Force Base Massachusetts 01731		10. PROGRAM ELEMENT, PROJECT, TASK AREA & WORK UNIT NUMBERS 62101F 66701012
14. MONITORING AGENCY NAME & ADDRESS (if different from Controlling Office)		12. REPORT DATE 13 December 1983
		13. NUMBER OF PAGES 44
		15. SECURITY CLASS. (of this report) Unclassified
		15a. DECLASSIFICATION DOWNGRADING SCHEDULE
16. DISTRIBUTION STATEMENT (of this Report) Approved for public release; distribution unlimited.		
17. DISTRIBUTION STATEMENT (of the abstract entered in Block 20, if different from Report)		
18. SUPPLEMENTARY NOTES		
19. KEY WORDS (Continue on reverse side if necessary and identify by block number) Short-range forecasting Objective forecasting Meteorology Mesoscale analysis Aviation weather		
20. ABSTRACT (Continue on reverse side if necessary and identify by block number) → This report describes a series of three experiments designed to test the feasibility of using upper-level steering of weather patterns to produce short-range local forecasts. Objective forecast models were developed and tested using fall and winter data from northeastern United States. The complexity of the models was increased in attempts to treat problems related to coexistence of stationary and traveling patterns and the effects of diurnal changes in the boundary layer. The first model simply steers (or "advects") aviation weather para-		

DD FORM 1 JAN 73 1473 EDITION OF 1 NOV 65 IS OBSOLETE

Unclassified

SECURITY CLASSIFICATION OF THIS PAGE (When Data Entered)

Unclassified

SECURITY CLASSIFICATION OF THIS PAGE (When Data Entered)

cont

meters analyzed on an x-y grid by looking upstream at 1-hour time steps. The model was tested during a 3-week period using the AFGL McIDAS facility, preparing 0-15-hour forecasts of wind, cloud cover, visibility, and dewpoint at three locations. Two steering flows used were the 700-mb wind field and the vertically integrated 850- to 300-mb wind field. In general, the root-mean-square (rms) errors were worse than persistence for 0-9 hours. Because errors were introduced when stationary (orographic) patterns were advected together with traveling systems, the forecast model was revised to advect the change-with-time fields. This model was tested on 12 winter cases. Scores for vector wind, cloud amount, and temperature were slightly better than both persistence and model-output-statistics (MOS) at 0-3 hours, but were worse at longer periods. One difficulty was that the diurnal changes reversed sign several hours into the forecast.

A third model was developed that treats the diurnal changes separately. This model was tested on 12 days in March, producing forecasts of wind, cloud cover, visibility, temperature, and dewpoint at 12 stations. The results indicate that most of the improvement achieved by the change-advection model is due to successful extrapolation of diurnal changes. In addition, the improvements over persistence are larger when the cases are "active-looking," that is, when the horizontal gradients are large.

When the complexity of the models was increased, skill scores with respect to persistence did improve, but much remains to be accomplished before operational testing would be justified. High frequency noise (particularly in surface winds) must be filtered, perhaps by using running-time averages. A systematic initialization scheme, including error checking and correction of biases caused by instrument exposure, is needed. Finally, the McIDAS objective routine used a 1-degree latitude-longitude grid with but a single pass, and large time-zero interpolation error indicated that higher resolution, multiple-pass analysis schemes would be preferred.



Accession For	
NTIS GRA&I	<input checked="checked" type="checkbox"/>
DTIC TAB	<input type="checkbox"/>
Unannounced	<input type="checkbox"/>
Justification	
By	
Distribution/	
Availability Codes	
Dist	Avail and/or Special
A-1	

DTIC
ELECTE
S JUL 20 1984 D
B

Unclassified

SECURITY CLASSIFICATION OF THIS PAGE (When Data Entered)

Contents

1. INTRODUCTION	5
2. ADVECTION EXPERIMENT I	7
3. ADVECTION EXPERIMENT II	10
4. ADVECTION EXPERIMENT III	16
5. CONCLUSIONS AND DISCUSSION	41
REFERENCES	43

Illustrations

1a. RMS Temperature Errors vs Forecast Time, Advection Forecast Experiment II	14
1b. Temperature Bias vs Forecast Time, Advection Forecast Experiment II	15
2. Mean Temperature vs Time of Day, 4 Canadian Stations, March	19
3. Mean Temperature Departure vs Time of Day, 3 Cloud Conditions, March	20
4. Mean Wind Speed Departure vs Time of Day, 3 Cloud Conditions, March	21
5a. RMS Wind Vector vs Forecast Time, Advection Forecast Experiment III, 700-500S Flow	30

5b. RMS Wind Speed vs Forecast Time, Advection Forecast Experiment III, 700-500S Flow	31
5c. RMS Cloud Amount vs Forecast Time, Advection Forecast Experiment III, 700-500S Flow	32
5d. RMS Ln Visibility vs Forecast Time, Advection Forecast Experiment III, 700-500S Flow	33
5e. RMS Temperature vs Forecast Time, Advection Forecast Experiment III, 700-500S Flow	34
5f. RMS Dewpoint vs Forecast Time, Advection Forecast Experiment III, 700-500S Flow	35
6a. Persistence Bias vs Forecast Time, Wind Speed, Advection Forecast Experiment III	36
6b. Persistence Bias vs Forecast Time, Cloud Amount, Advection Forecast Experiment III	37
6c. Persistence Bias vs Forecast Time, Ln Visibility, Advection Forecast Experiment III	38
6d. Persistence Bias vs Forecast Time, Temperature, Advection Forecast Experiment III	39
6e. Persistence Bias vs Forecast Time, Dewpoint, Advection Forecast Experiment III	40

Tables

1. Advection Forecast Experiment I, Skill Scores Relative to Persistence	9
2. Advection Forecast Experiment II, Skill Scores Relative to Persistence	12
3a. Advection Forecast Experiment III, Skill Scores Relative to Persistence, Vector Wind	24
3b. Advection Forecast Experiment III, Skill Scores Relative to Persistence, Wind Speed	25
3c. Advection Forecast Experiment III, Skill Scores Relative to Persistence, Cloud Cover	26
3d. Advection Forecast Experiment III, Skill Scores Relative to Persistence, Visibility	27
3e. Advection Forecast Experiment III, Skill Scores Relative to Persistence, Temperature	28
3f. Advection Forecast Experiment III, Skill Scores Relative to Persistence, Dewpoint	29

Experiments in Objective Aviation Weather Forecasting Using Upper-Level Steering

1. INTRODUCTION

When winds-aloft data became routinely available to meteorologists, the forecasters quickly noted the similarity between the motion of storm systems and the air flow at levels of 3-6 km (500-700 mb). This relationship became the basis for 12- to 24-hour forecasting using "upper-level steering." This practice received physical justification when barotropic theory was developed, particularly when Fjörtoft¹ applied the theory to forecasting in the form of a graphical 500-mb forecast technique, using a space-averaged flow for steering vorticity parcels (or "advecting" the parcels). Soon after, Estoque² and Reed³ developed graphical 1000-mb forecast techniques, applying baroclinic theory, and these techniques steered thermal patterns using upper-level wind flow.

During the 1970s, the fine-mesh numerical forecast products improved so that they now serve as the basis for virtually all prognostic charts, and the steering

(Received for publication 7 December 1983)

1. Fjörtoft, R. (1952) On a numerical method of integrating the barotropic vorticity equation, Tellus 4:179-194.
2. Estoque, M.A. (1957) A graphical integration of a two-level model, J. Atmos. Sci. 14:38-42.
3. Reed, R.J. (1960) On the practical use of graphical prediction methods, Mon. Wea. Rev. 88:209-218.

techniques have become obsolete. Unfortunately, even the latest fine-mesh numerical model uses a grid of about 190 km. Consequently, the weather disturbances in the model are fairly large, producing gradual changes over periods of 15-30 hours or more. This has left the local forecaster on his own to predict the more rapid weather changes that occur over periods of several hours. Many of these rapid changes are associated with the passage of surface fronts and troughs or with the arrival of clouds and precipitation, phenomena that, in mid-latitudes, are closely related to the traveling cyclones and anticyclones. Since the upper-level steering principle once served well in forecasting the motion of cyclones and anticyclones, a natural deduction would be that steering would also work for the finer scale "sub-synoptic" scale disturbances associated with the cyclones and anticyclones.

In fact, some indication exists that upper-level steering can be used with small-scale disturbances. In a forecast test, Muench⁴ used objectively determined motion vectors as well as 700-mb and 500-mb winds to make objective short-range forecasts of cloudiness and precipitation, using geosynchronous satellite imagery. The test showed marked improvement over persistence for forecasts more than 2 hours, with nearly equal skill for the objective motion vector and the two upper-level winds. When the size of the cloud and precipitation patterns in typical satellite images and radar displays is taken into account, the test must be considered as at least partial verification of the concept of upper-level steering for small- or "meso-" scale disturbances.

While the satellite data are nearly ideal for cloud cover prediction and the IR-visible channel combination can specify precipitation areas fairly well, a number of other weather parameters that cannot be easily related to satellite measurements are of interest to aviation forecasters. In particular, ceiling, visibility, and surface wind are very important to operations, and forecasts of altimeter setting, temperature, and humidity are sometimes needed. To use steering for objective forecasts of these parameters, one would have to use the hourly aviation weather reports to define the patterns and the radiosonde data to define the upper-level winds.

To test the feasibility of using the steering concept for objective short-range terminal forecasts, several forecast models of increasing complexity were developed and tested. This report will describe these steering or advection models, the tests that were performed, and the conclusions that can be drawn from the tests.

4. Muench, H.S. (1981) Short-Range Forecasting of Cloudiness and Precipitation Through Extrapolation of GOES Imagery, AFGL-TR-81-0218, AD A108678.

2. ADVECTION EXPERIMENT 1

By the fall of 1981, the AFGL McIDAS facility had the means to make tests of the steering or advection technique for surface weather parameters. Hourly weather observations and radiosonde ascents have been routinely saved on disk storage and dumped to magnetic tape twice a week. Software developed by the University of Wisconsin was installed that performed objective analyses of almost any parameter, developing grid-point values from irregularly spaced observations. In addition, a routine had been written⁵ that computed locations of upstream trajectories of upper-level winds, at 1-hour intervals, and that sought out the corresponding weather parameter from another grid field to produce advection forecasts.

In mathematical terms, if a quantity X is conservative for some given horizontal flow field, we can write

$$\frac{dX}{dt} = 0$$

which becomes

$$\frac{\partial X}{\partial t} = -V^* \frac{\partial X}{\partial S} \quad (1)$$

where V^* is the advecting wind speed along the streamline S (or steering current). If Eq. (1) is integrated from time $t = 0$ to $t = t$, starting at location $x = 0$, $y = 0$, we have $X_{00t} - X_{000} = X_{xyt} - X_{000}$ or $X_{00t} = X_{xy0}$, which means that the forecast for $x = 0$, $y = 0$, $t = t$ is simply the upstream value of X at $x = x$, $y = y$, $t = 0$ (or the initial time).

Using the same notation, a forecast of "persistence" means

$$\frac{\partial X}{\partial t} = 0 \text{ or } X_{00t} = X_{000} \quad (2)$$

A 3-week test of the advection forecast technique was conducted from mid-October to early November 1981, using the McIDAS facility. Three stations were chosen: Boston, Mass.; Burlington, Vt.; and Atlantic City, N. J. Forecasts were made from 00 GMT radiosonde and 03 GMT surface data, and again from 12 GMT radiosonde and 15 GMT surface data. Advection forecasts were made for the u and

5. Wash, C.H., and Whittaker, T.M. (1980) Subsynoptic analysis and forecasting with an interactive computer system, Bull. Am. Meteorol. Soc. 61:1584-1591.

v components of the surface wind, the total cloud cover (including "thin"), visibility, and dewpoint. While the McIDAS routine made hourly forecasts out to 15 hours in 1-hour steps, only the 0-, 1-, 2-, 3-, 9-, and 15-hour forecasts were recorded, providing adequate time coverage and simple verification.

In addition to persistence, model-output-statistics (MOS) forecasts⁶ were also used as a control. The corresponding MOS forecasts were collected from the Air Force COMEDS circuit for the 3-, 9-, and 15-hour periods. These MOS forecasts have compared favorably with local subjective forecasts of 12-36 hours.⁷ The forecasts are based on data from the NMC LFM model prediction together with data from a local observation taken 3 hours after the initial data for the LFM. Statistically derived relationships combine the data into forecasts of a wide variety of weather parameters.

In the verifications for this study, the standard of comparison is the root-mean-square error (rms error). The rms error was chosen rather than the mean-absolute-error (MAE) on the presumption that emphasis should be given to reducing the largest errors. In general, the rms errors are about 25-30 percent larger than MAEs. In some cases when the skill scores are within ± 10 percent of zero, the scores based on rms error may be of opposite sign to those based on MAE, but normally the skill scores are similar. The cloud amount and visibility scores were based on the MOS categories and thus represent rms category errors. The scores for wind were the rms vector error (combining u and v component errors), and the dewpoint scores were simply rms errors. More details of this experiment may be found in the Appendix of Muench.⁴ Two different advecting wind fields were used, the 700-mb wind and the 850-300-mb vertically averaged wind.

Results of Advection Experiment I are summarized in Table 1, and show the rms errors for persistence and the skill scores relative to persistence [skill = (persistence error-forecast error)/persistence error]. Overall, the results were somewhat disappointing and difficult to understand. For wind, cloud amount, and dewpoint, the only positive scores (underlined values), representing improvement over persistence, were for periods beyond 3 hours, and even these were less accurate than the MOS forecasts. If the steering field were changing with time or if the weather patterns were undergoing significant development or decay, then the shorter period forecasts should have been more accurate than the longer period forecasts; instead, we see the reverse here. Only the visibility forecasts for 2 and

6. Glahn, H.R., and Lowry, D. (1972) The use of model output statistics (MOS) in objective weather forecasting, J. Appl. Meteorol. 11:1203-1211.

7. Zurndorfer, E.A.; Bocchieri, J.R.; Carter, G.M.; Dallaville, J.P.; Gilhausen, D.B.; Hebenstreit, K.F.; Vercelli, D.J. (1979) Trends in comparative verification scores for guidance and local aviation weather forecasts, Mon. Wea. Rev. 107:799-811.

Table 1. Advection Forecast Experiment I, Skill Scores Relative to Persistence

Technique/Time (h)	Wind (rms vector error)					
	0	1	2	3	9	15
Persistence	(±0.00)	(±1.88)	(±2.72)	(±3.18)	(±3.89)	(±6.11)
Advection 700 mb	(±2.39)	-0.60	-0.18	-0.08	<u>+0.15</u>	<u>+0.21</u>
Advection 850-300 mb	(±2.39)	-0.68	-0.20	-0.09	<u>+0.12</u>	<u>+0.20</u>
AWS-MOS	xxx	xxx	xxx	<u>+0.05</u>	<u>+0.31</u>	<u>+0.29</u>
Technique/Time (h)	Cloud Cover (rms category error, 0-3)					
	0	1	2	3	9	15
Persistence	(±0.00)	(±0.36)	(±0.50)	(±0.81)	(±1.11)	(±1.22)
Advection 700 mb	(±0.73)	-1.17	-0.84	-0.84	<u>+0.08</u>	-0.08
Advection 850-300 mb	(±0.73)	-1.14	-0.80	-0.69	<u>+0.00</u>	-0.16
AWS-MOS	xxx	xxx	xxx	-0.19	<u>+0.1</u>	<u>+0.27</u>
Technique/Time (h)	Visibility (rms category error, 0-4)					
	0	1	2	3	9	15
Persistence	(±0.00)	(±0.47)	(±0.76)	(±0.83)	(±1.1)	(±1.18)
Advection 700 mb	(±0.48)	-0.45	<u>+0.08</u>	<u>+0.00</u>	-0.	<u>+0.06</u>
Advection 850-300 mb	(±0.48)	-0.38	<u>+0.01</u>	<u>+0.02</u>	-0.1	<u>+0.09</u>
AWS-MOS	xxx	xxx	xxx	<u>+0.10</u>	<u>+0.00</u>	<u>+0.11</u>
Technique/Time (h)	Dewpoint Temperature (rms error, Celsius)					
	0	1	2	3	9	15
Persistence	(±0.00)	(±0.70)	(±1.55)	(±2.18)	(±3.45)	(±4.93)
Advection 700 mb	(±1.61)	-1.74	-0.41	-0.16	-0.08	<u>+0.03</u>
Advection 850-300 mb	(±1.61)	-1.80	-0.48	-0.23	-0.31	<u>+0.06</u>
AWS-MOS	xxx	xxx	xxx	xxx	xxx	xxx

3 hours show promise, and these skill levels are less than MOS. The positive skill scores at the longer times indicate that some features are being properly advected, and the negative scores at shorter periods must mean that some features of small size (or short lifetime) are being improperly advected, wiping out some gains (albeit small) over persistence.

There are three principal ways that anomalous features might appear in the analyzed fields, leading to erroneous forecasts. First, there are the inevitable observational errors in making judgments about visibility and cloud cover, or in determining winds and dewpoints from strip-charts or dials. These errors are likely to be as high as 60 percent of the rms 1-hour change or persistence error.

Another way is smoothing some features. The analysis procedure consists of a single Cressman-type grid-point analysis⁸ on a 1-degree longitude-latitude grid

8. Cressman, G. P. (1959) An operational objective analysis system, Mon. Wea. Rev. 87:367-371.

(usually 15 by 33 degrees) and, admittedly, does oversmooth some important small-scale features (see Gerlach⁹). This smoothing accounts for many of the zero hour rms errors seen in parentheses in Table 1. These errors represent the inability of the interpolation routine to recover the initial values of the observations from the grid-point values. While one would certainly prefer better analyses, perhaps a three-pass Barnes-type analysis¹⁰ on 1/2-degree grids, such a program would have overtaxed the computational capabilities of the McIDAS if performed on the 15 by 33-degree area necessary for trajectories out to 15 hours.

The third potential source of error is the presence of standing or stationary disturbances in the otherwise moving weather patterns. Orographically related cloud patterns were known to have degraded some of the forecasts in the satellite-based forecast of Muench,⁴ and forecasters are quite familiar with such features as lee-side wind (and pressure) troughs, coastal convergence zones, and systematic lowering of visibility with altitude (in poor weather). Any forecast procedure that attempted to advect these stationary disturbances would certainly suffer from increased forecast errors.

3. ADVECTION EXPERIMENT 11

The first modification of the advection routine was an attempt to reduce errors incurred when stationary disturbances were advected. To begin, the predictand X is now assumed to be composed of two components, a stationary or orographic component \hat{X} and a moving component X' . Thus $X = \hat{X} + X'$. The local time derivative is

$$\frac{\partial X}{\partial t} = \frac{\partial \hat{X}}{\partial t} + \frac{\partial X'}{\partial t}$$

We now assume that $\partial X / \partial t = 0$ (or at least is negligible compared with $\partial X' / \partial t$). As before, we assume the moving pattern (now X') is conservative or $dX' / dt = 0$. This also means that $d/dt (\partial X' / \partial t) = 0$. Since $\partial \hat{X} / \partial t = 0$ everywhere and for all time, we can write $d/dt (\partial \hat{X} / \partial t) = 0$. Thus

$$\frac{d}{dt} \left(\frac{\partial X}{\partial t} \right) = \frac{d}{dt} \left(\frac{\partial X'}{\partial t} + \frac{\partial \hat{X}}{\partial t} \right) = 0$$

9. Gerlach, A., ed. (1982) Objective Analysis and Prediction Techniques, AFGL-TR-82-0394, AD A131465.

10. Barnes, S.L. (1964) A technique for maximizing details in numerical weather map analyses, J. Appl. Meteor. 3:396-409.

This now means that $(\partial X / \partial t)$ is conservative, and we can write

$$\frac{\partial}{\partial t} \left(\frac{\partial X}{\partial t} \right) = -v \cdot \frac{\partial}{\partial s} \left(\frac{\partial X}{\partial t} \right) \quad (3)$$

Integrating over time (advecting $\partial X / \partial t$), we have

$$\left(\frac{\partial X}{\partial t} \right)_{00t} - \left(\frac{\partial X}{\partial t} \right)_{000} = \left(\frac{\partial X}{\partial t} \right)_{xy0} - \left(\frac{\partial X}{\partial t} \right)_{000} \quad \text{or} \quad \left(\frac{\partial X}{\partial t} \right)_{00t} = \left(\frac{\partial X}{\partial t} \right)_{xy0}$$

A second integration and converting an integration to a finite difference summation yields

$$X_{00t} - X_{000} = \frac{1}{\Delta t} \sum (X_{xy0} - X_{xy-\Delta t})$$

The new forecast equation is then

$$X_{00t} = X_{000} + \frac{1}{\Delta t} \sum (X_{xy0} - X_{xy-\Delta t}) \quad (4)$$

that we will call the "change-advection" forecast technique. Following the lead of early synoptic meteorologists, who adopted 3 hours to compute pressure tendency, we chose 3 hours for Δt . This forecast equation has the desirable feature of starting with the observed weather at the forecast site at time zero, thus incorporating some local effects and starting on an equal footing with persistence.

A feasibility test of the change-advection technique was conducted for 12 cases from early December 1982 through March 1983. The cases were not random; nearly all involved major storm systems in the eastern United States that had appreciable motion and that were likely to contain mixtures of stationary and moving patterns. In this test, forecasts were again made for surface wind and cloud cover. However, this time, temperature replaced dewpoint for a test of how both advection and change-advection scored on a parameter with an important diurnal component. Again, 700-mb flow was used for an advective wind, but now the 700-500-mb vertically averaged wind was given a spatial smoothing through several passes of a simple 5-point averaging routine (called "filter" on McIDAS). In the previous test, frontal zones had not been forecast eastward fast enough, probably because of changing steering currents, and it was hoped that this smoothing (analogous to the Fjörtoft \bar{Z} field) might correct the problem. It was felt that 700-mb and 500-mb winds provided sufficient information on vertical structure and would produce a

vertical average wind nearly identical to the 850-300-mb mean used in Experiment I.

For this test, the number of stations was increased to six, including Boston, Mass.; Philadelphia, Pa.; Washington, D.C., National Airport; Buffalo, N.Y.; Pittsburgh, Pa., and Columbus, Ohio. Four advection forecasts were made: 700 mb advection, 700-500 mb (filtered) advection, 700 mb change-advection, and 700-500 mb (filtered) change-advection. Persistence and the NMC MOS forecasts (then available on McIDAS through new software⁹) were controls. Forecasts were made for 0, 1, 2, 3, 6, 9, 12, and 15 hours, with the 6- and 12-hour forecasts added to better define where the positive skill scores began. Six cases were based on 00-03 GMT data, and six on 12-15 GMT data. Again, rms errors were computed to use as a basis for comparing scores. The results of Experiment II are summarized in Table 2 (in the same format as Table 1).

Overall, the results of this experiment were encouraging. For the winds, we note that there were modest positive skill-scores for simple advection starting at

Table 2. Advection Forecast Experiment II, Skill Scores Relative to Persistence

VECTOR WIND (rms error, mps, in parentheses)								
TECHNIQUE/TIME (H)	0	1	2	3	6	9	12	15
Persistence	(±0.00)	(±2.01)	(±2.43)	(±2.71)	(±4.30)	(±5.21)	(±6.04)	(±6.25)
Advection 700mb	(±1.51)	-0.01	-0.11	<u>+0.05</u>	<u>+0.23</u>	<u>+0.32</u>	<u>+0.28</u>	<u>+0.31</u>
Advection 7-5F	(±1.51)	-0.10	-0.09	<u>+0.03</u>	<u>+0.26</u>	<u>+0.31</u>	<u>+0.29</u>	<u>+0.28</u>
Chng Adv. 700mb	(±0.00)	<u>+0.00</u>	<u>+0.00</u>	-0.15	-0.06	<u>+0.00</u>	<u>+0.05</u>	<u>+0.00</u>
Chng Adv. 7-5F	(±0.00)	<u>+0.00</u>	<u>+0.03</u>	-0.13	-0.08	-0.07	-0.03	-0.11
NMC-MOS	(±0.00)	xxx	xxx	-0.05	xxx	<u>+0.44</u>	xxx	<u>+0.47</u>
TOTAL CLOUD AMOUNT (rms category error, 0-3)								
TECHNIQUE/TIME (H)	0	1	2	3	6	9	12	15
Persistence	(±0.00)	(±0.50)	(±0.60)	(±0.70)	(±1.00)	(±1.10)	(±1.30)	(±1.50)
Advection 700mb	(±0.55)	-0.60	-0.17	-0.05	-0.15	-0.09	-0.05	<u>+0.03</u>
Advection 7-5F	(±0.55)	-0.50	-0.17	-0.14	-0.10	-0.09	<u>+0.08</u>	<u>+0.00</u>
Chng Adv. 700mb	(±0.00)	<u>+0.10</u>	<u>+0.08</u>	<u>+0.29</u>	<u>+0.10</u>	-0.05	<u>+0.00</u>	<u>+0.00</u>
Chng Adv. 7-5F	(±0.00)	-0.20	<u>+0.00</u>	<u>+0.00</u>	<u>+0.05</u>	<u>+0.00</u>	<u>+0.04</u>	-0.03
NMC-MOS	(±0.00)	xxx	xxx	-0.29	xxx	<u>+0.09</u>	xxx	<u>+0.27</u>
TEMPERATURE (rms error, Celsius, in parentheses)								
TECHNIQUE/TIME (H)	0	1	2	3	6	9	12	15
Persistence	(±0.00)	(±0.86)	(±1.45)	(±1.96)	(±2.75)	(±3.17)	(±3.63)	(±4.33)
Advection 700mb	(±0.92)	-0.74	-0.55	-0.51	-0.13	-0.01	-0.23	-0.32
Advection 7-5F	(±0.92)	-0.74	-0.53	-0.48	-0.35	-0.12	-0.15	-0.09
Chng Adv. 700mb	(±0.00)	<u>+0.19</u>	<u>+0.17</u>	<u>+0.18</u>	-0.01	-1.09	-1.10	-1.26
Chng Adv. 7-5F	(±0.00)	<u>+0.19</u>	<u>+0.17</u>	<u>+0.20</u>	<u>+0.04</u>	-0.48	-1.09	-1.25
NMC-MOS	(±0.00)	xxx	xxx	<u>+0.15</u>	<u>+0.20</u>	<u>+0.32</u>	<u>+0.41</u>	<u>+0.48</u>

3 hours, and, compared to Experiment I, the scores are higher. The change-advection scores are better than simple advection at 1 and 2 hours, but worse than advection for longer periods. One should note that the forecast skill scores for MOS are also higher for this test than for Experiment I, suggesting that the wind patterns in these selected cases were moving more predictably.

The cloud amount forecasts for advection had positive skill scores only for the longest time periods, consistent with the Experiment I results. However, the change-advection technique shows positive skill for the 1-4-hour period, at least for 700 mb steering. Since this test was based on selected cases similar to those in the test using satellite imagery,⁴ we might have expected to see advection better than persistence beyond 2 hours. The relatively poor performance of simple advection using only airways observations for periods less than 12 hours suggests there is a great advantage in using satellite imagery to forecast cloud amount objectively, no doubt due to the much higher spatial resolution.

The skill scores for temperature indicate features that might well have been anticipated. The advection forecasts are worse than persistence for all time periods, with much of the error resulting from attempts to advect the orographically reduced temperatures of mountain stations within the Appalachian region. Also, some of the stations in this test are "heat island" stations, with local anomalies that do not move. As might be expected, the change advection skill scores are much better (at least for 1-3 hours) and certainly look encouraging. Unfortunately, the change-advection forecasts have very poor skill scores beyond 6 hours and appear to "blow up."

An immediate suspicion is that all the change-advection routine is really doing with temperature is extrapolating the diurnal change of the previous 3 hours (averaged spatially) out to 15 hours, hour by hour. During the first few hours, the forecasts benefit by this extrapolation as the diurnal trend continues, but, before long, the real trend reverses and the forecasts are useless.

A further indication of the effects of the diurnal temperature change can be seen in Figures 1a and 1b. These figures depict the rms errors and the mean-arithmetic-errors (or bias) for 15-GMT forecasts. The rapid increase in change-advection rms error beyond 6 hours is very evident in Figure 1a. In Figure 1b, it is equally evident that nearly all of this increase is the result of the nearly linear increase in the bias. In fact, the relative standings of all three forecast techniques in Figure 1a are essentially determined by the relative size of the bias errors at all time periods. One should note that the diurnal temperature rise (negative persistence bias) from 15 GMT to 18 GMT was only +1.4° C. This temperature rise is less than the normal for this region in winter and reflects effects of the extensive cloud cover for these 12 cases. And, of course, the winter diurnal is smaller than the diurnal for the other seasons, when solar heating is stronger. Neverthe-

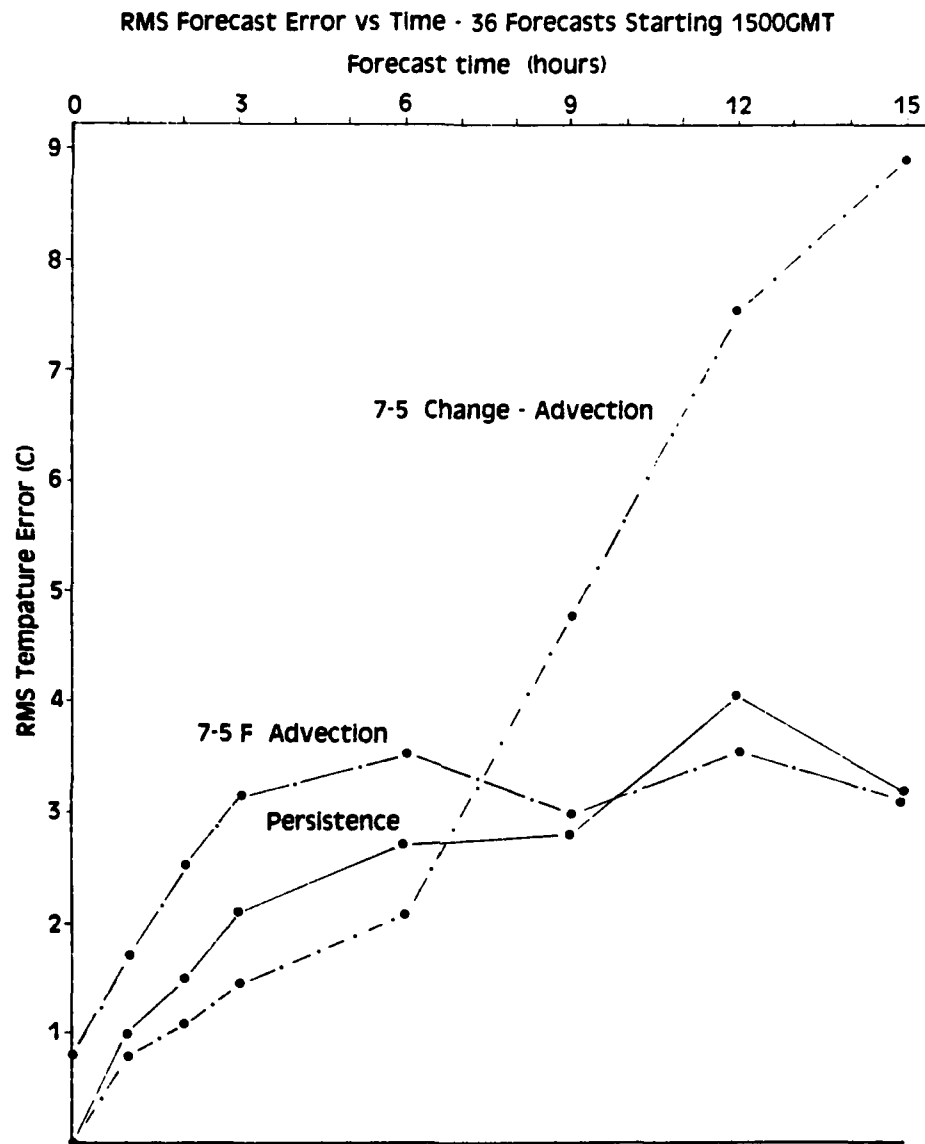


Figure 1a. RMS Temperature Errors vs Forecast Time, Advection Forecast Experiment II

less, even in winter, the diurnal heating cycle plays a very important role in the short-range temperature forecasts.

A last point is that the skill scores in Table 2 do not, overall, indicate any obvious advantage to either 700 mb steering or to the vertical-and-space-averaged flow (7-5F). The differences between the skill scores of these two are small and

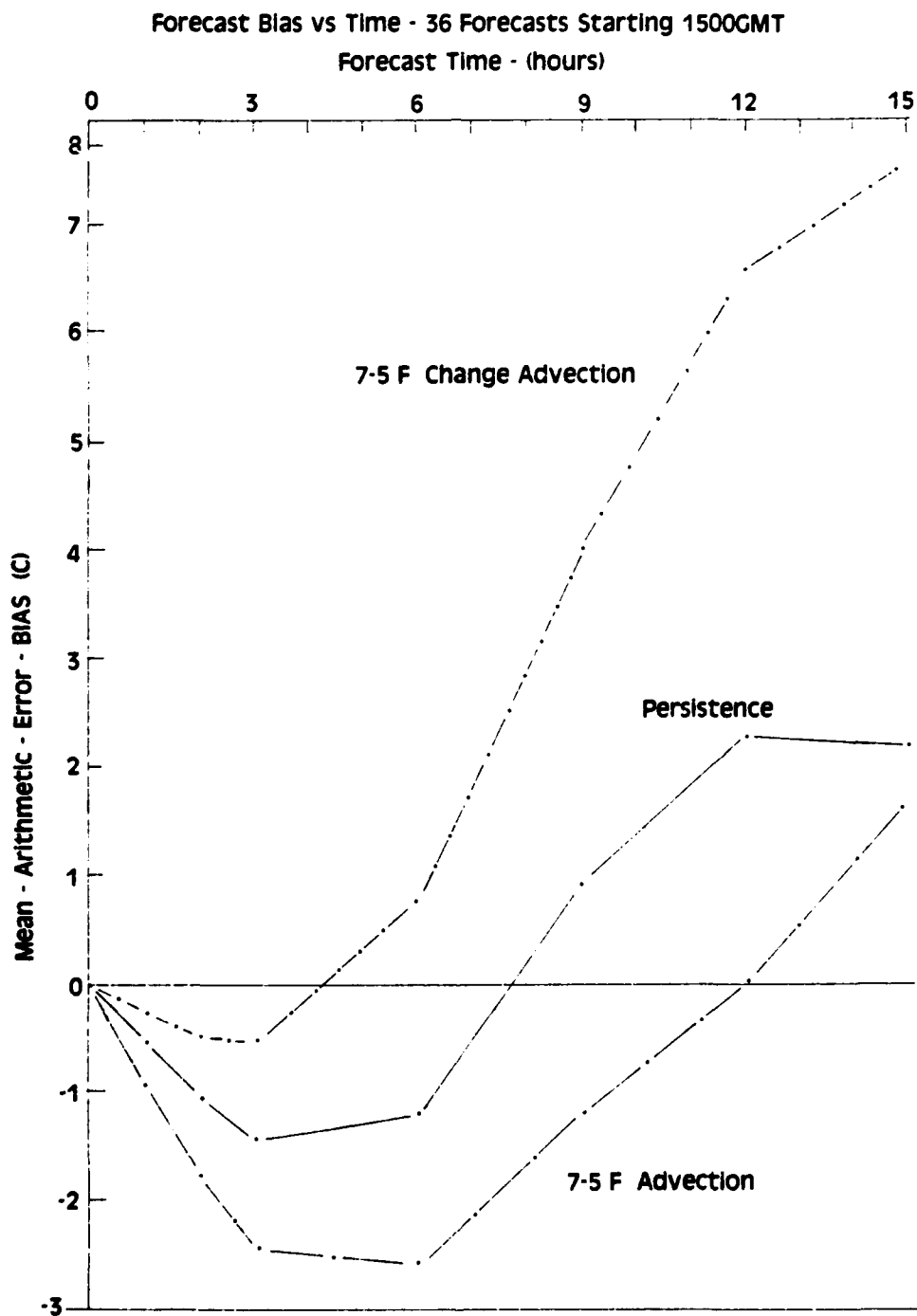


Figure 1b. Temperature Bias vs Forecast Time, Advection Forecast Experiment II

do not seem to be consistent over all time periods. Based on these results, there is little to choose between these two.

4. ADVECTION EXPERIMENT III

The effects of the diurnal temperature changes on the accuracy of the advection techniques were to be expected. One would not realistically attempt to develop a temperature forecast technique without allowing for the diurnal. Radiative heating and cooling directly cause the temperature change; the temperature change, in turn, affects the relative humidity; and the humidity, in turn, affects the visibility and the cloud ceiling height. The temperature change also affects the hydrostatic stability that, in turn, affects turbulent exchange and the surface wind speed. Thus, several other parameters also have diurnal changes, even though the changes might not be as marked as the daily temperature cycle. In the change-advection forecasts, small diurnal changes become amplified as each iteration is carried out. For these reasons, one of the first steps in developing Advection Model III was to re-derive the forecast equations to include diurnal changes.

To start, we now say $X = \tilde{X} + \hat{X} + X'$, where the diurnal component is indicated by \tilde{X} . To obtain a persistence forecast with diurnal modification (persistence + diurnal), we assume, as before, $\partial \hat{X} / \partial t = 0$ and $\partial X' / \partial t = 0$, and we are left with $\partial X / \partial t = \partial \tilde{X} / \partial t$. Integrating this last expression over time, the forecast expression becomes

$$X_{00t} = X_{000} - \tilde{X}_{000} + \tilde{X}_{00t} \quad (5)$$

Simply put, the persistence + diurnal forecast consists of the present value minus the present diurnal component plus the future diurnal component.

To obtain the expression for advection forecast modified for diurnal effect (advection + diurnal), we start with $X = \tilde{X} + X'$ (assuming $\hat{X} = 0$). Since X' is defined as the traveling component and is assumed to be conservative, we see that $dX/dt = d\tilde{X}/dt$ or $d(X - \tilde{X})/dt = 0$. Since $(X - \tilde{X})$ is conservative, we have $\partial(X - \tilde{X})/\partial t = -V \cdot \partial(X - \tilde{X})/\partial s$. Integrating this expression over time, we have the following forecast equation:

$$X_{00t} = X_{xy0} - \tilde{X}_{xy0} + \tilde{X}_{00t} \quad (6)$$

The addition of the diurnal term does complicate the change-advection forecast equation. To derive a change-advection + diurnal formula, we start with a conserv-

ative equation $d/dt (\partial X / \partial t - \partial \tilde{X} / \partial t) = 0$, from which we derive

$$\frac{\partial}{\partial t} \left(\frac{\partial X}{\partial t} - \frac{\partial \tilde{X}}{\partial t} \right) = -v * \frac{\partial}{\partial s} \left(\frac{\partial X}{\partial t} - \frac{\partial \tilde{X}}{\partial t} \right)$$

After the necessary integrations over time, the forecast equation is found to be

$$X_{00t} = X_{000} - \tilde{X}_{000} + \frac{1}{\Delta t} \sum (X_{xy0} - \tilde{X}_{xy0} - X_{xy-\Delta t} + \tilde{X}_{xy-\Delta t}) + \tilde{X}_{00t} \quad (7)$$

These new forecast equations reached the state of complexity where a complete test using the McIDAS facility would have required extensive software development and modification. Thus, a new procedure was established: analyzed grid-fields for upper level winds and surface weather parameters were computed on McIDAS and then placed on magnetic tape for further processing on the AFGL CDC computers. In addition, the history file of hourly surface reports was copied onto magnetic tape, to be used later in the forecasts and verification. This new procedure was more fully automated and enabled forecasts to be made for more stations. The software used for decoding the tapes has potential use for future routines such as error checking, data filtering, and use with large scale, high resolution objective analysis programs.

In the discussion of the results of Experiment II (Section 3), there are suggestions that some of the improvement in the advection scores over the first test resulted from the choice of cases. The advection procedure may very well score better relative to persistence on large, steadily moving storm systems. The plan for Experiment III was to test the forecast techniques in a more routine fashion, taking on all weather situations as they arose.

The month of March 1983 was selected for the test because the data sets were more complete for that month than those gathered during the preceding months. Six new forecast stations were added to those of Experiment II: Windsor Locks, Conn.; Allentown, Pa.; Flint, Mich.; Cleveland, Ohio; Covington, Ky.; and Rome AFB, N.Y. Forecasts were computed and verified for all hours from 0-15 hours, even though most MOS forecasts were only made for 3, 9, and 15 hours (temperature and dewpoint are every 3 hours in NMC-MOS). The forecast parameters included vector wind, wind speed, cloud amount, visibility, temperature, and dewpoint. Visibility was converted to the natural log of visibility (LnV) to place more emphasis on the numerically small changes (and errors) that occur at the low end of the visibility range and that are so operationally important. Actually, the category ranges in the MOS forecasts for visibility are approximately logarithmic in their distribution. In addition to the vector wind, the wind speed was added as a

separate forecast parameter, obtained numerically in the advection routines from the magnitude of forecast wind components.

Having the upper-level-wind grids available to the AFGL CDC 6600 computer allowed for developing more elaborate space-smoothing routines. A new space-smoothed steering field was created by starting with McIDAS-generated 2-degree latitude-longitude grids of 700-mb and 500-mb u and v components of the wind (United States east of 105 W). Then vertically integrated grids were computed using 60 percent of the 700-mb wind components and 40 percent of the 500-mb wind components (an approximate density weighting). The grids were then given an 8- by 6-point spatial smoothing. Finally, 1-degree u- and v-component grid fields were interpolated for use in the advection forecasts. This new steering field was designated the 700-500S (where S indicated space-smoothed), and became the third steering field in addition to the 700 mb and the 7-5F (or McIDAS filtered steering fields). With three steering fields, simple advection and change-advection, with and without diurnal modification, there were 12 different advection forecast techniques to test.

The derived forecast Eqs. (5), (6), and (7) were based on the assumption that the diurnal variations of the weather parameters would be specified. The task then is to produce algorithms that would specify the diurnal component of the variable under differing weather conditions. In particular, one looks for a specification in the form of $X = f(t) * g(X_1, X_2, \dots, X_n)$ where X_i represents the other variables that would affect the amplitude of the diurnal curve (that is, cloud cover affecting temperature diurnal range). Few climatological summaries contain data based on time of day, but some information was found in the following sources: Air Force Revised Uniform Summary of Station Weather Observations (RUSSWO);^{11, 12} National Weather Service Decennial Census of the United States Climate: Summary of Hourly Observations;¹³ and the Canadian Hourly Data Summaries.¹⁴ The only hourly mean monthly dry-bulb and wet-bulb temperatures were found in the Canadian Summaries, while hourly cloud frequency (four categories) values were taken from the Decennial Census. Otherwise, data presented in these summaries is in the form of 3-hour mean frequencies for a number of categories for variables such as ceiling, visibility, wind direction, and wind speed.

11. Revised Uniform Summary of Surface Weather Observations, A-F, U. S. Air Force, AWS (by station) (about 500 pages each, available through NTIS).
12. An Aid for Using the Revised Uniform Summary of Surface Weather Observations (RUSSWO's) (1983) USAF TAC/TN-83/001, Scott AFB, IL 62225.
13. Climatology of the United States No. 82-41, Decennial Census of United States Climate: Summary of Hourly Observations 1951-1960 (by station), Superintendent of Documents, U. S. GPO, Washington, D. C.
14. Hourly Data Summaries No. 1-84 (by station), Climatology Division Meteorological Branch, Department of Transport, Canada.

Some hourly temperature values for Canadian airports¹⁴ were extracted and are shown in Figure 2. The curves are fairly smooth. Therefore, 3-hour means would describe the overall features but would underestimate the amplitude because of the averaging. Also, there would be difficulties positioning the time of maximum and minimum.

Because of the lack of resolution in the 3-hour data and the difficulties working with frequencies (rather than mean values), and because the climatological values are functions of time only, more detailed diurnal information was developed by using the McIDAS archived hourly observations. A program extracted hourly reports from 80 stations east of 90 W from the archive tape for March 1983.

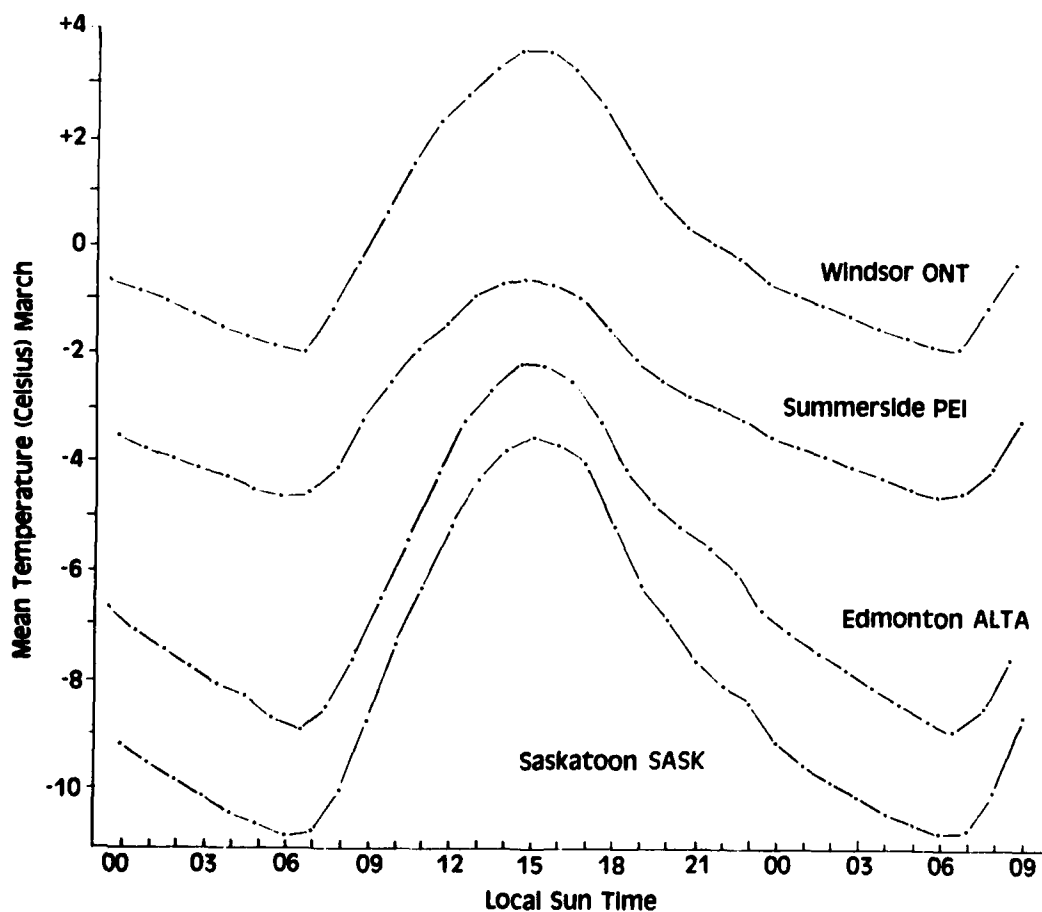


Figure 2. Mean Temperature vs Time of Day, 4 Canadian Stations, March

The mean values for 1-hour changes in wind speed, natural log of visibility ($\ln V$), and temperature were derived for a variety of initial weather conditions, including cloud cover (by amount and layer), wind speed, and dewpoint spread. To compute a diurnal curve, the first step was to subtract the 24-hour mean of the 1-hour changes from individual changes in order to remove any bias. For example, clear-sky cases may contain cooling due to advection. Next, a first-guess diurnal curve was constructed by integrating the 1-hour changes (bias removed) starting at 00 GMT. Because 00 GMT is rarely a null point, a phase correction was made by computing the 24-hour average and subtracting from individual values. Figures 3 and 4 show examples of diurnal curves for three different cloud conditions for temperature and wind speed. These curves represent the mean of all 80 stations.

The systematic differences in diurnal amplitude going from low-broken/-overcast are quite noticeable in Figures 3 and 4. In the case of temperature, the shapes and phase for all curves are similar, indicating that a fairly simple algo-

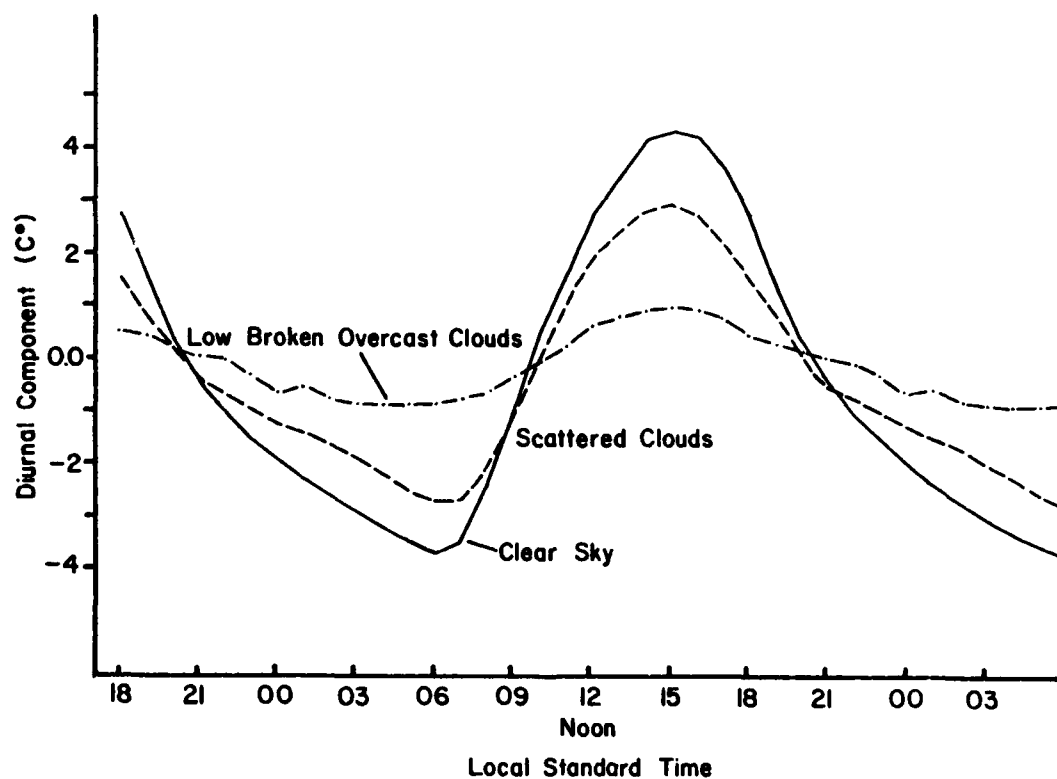


Figure 3. Mean Temperature Departure vs Time of Day, 3 Cloud Conditions, March

rithm of the form $\tilde{T} = f(t) g(\text{cloud})$ could be constructed. One problem is that the weather elements that affect diurnal cycles contain diurnal components themselves, and it is difficult to know where to begin. The simplest procedure seemed to be to start with the cloud cover. Cloud cover has a small diurnal amplitude compared to its dynamic changes and, consequently, neglect of diurnal feedback would not be serious. The following algorithms were developed, based on Decennial Census hourly cloud amount frequencies:¹³

$$\tilde{C} = C - \bar{C} = 0.3 * (30 - \bar{C}) * f(t) \quad (C > 10)$$

$$\tilde{C} = C - \bar{C} = 0.6 * \bar{C} * f(t) \quad (C \leq 10)$$

where \bar{C} is the non-diurnal cloud amount, which ranges from 0 for clear to 30 for overcast. If C and not \bar{C} is known, these equations can easily be solved to obtain C and \tilde{C} .

The March 1983 study based on 80 stations indicated that the strongest effect

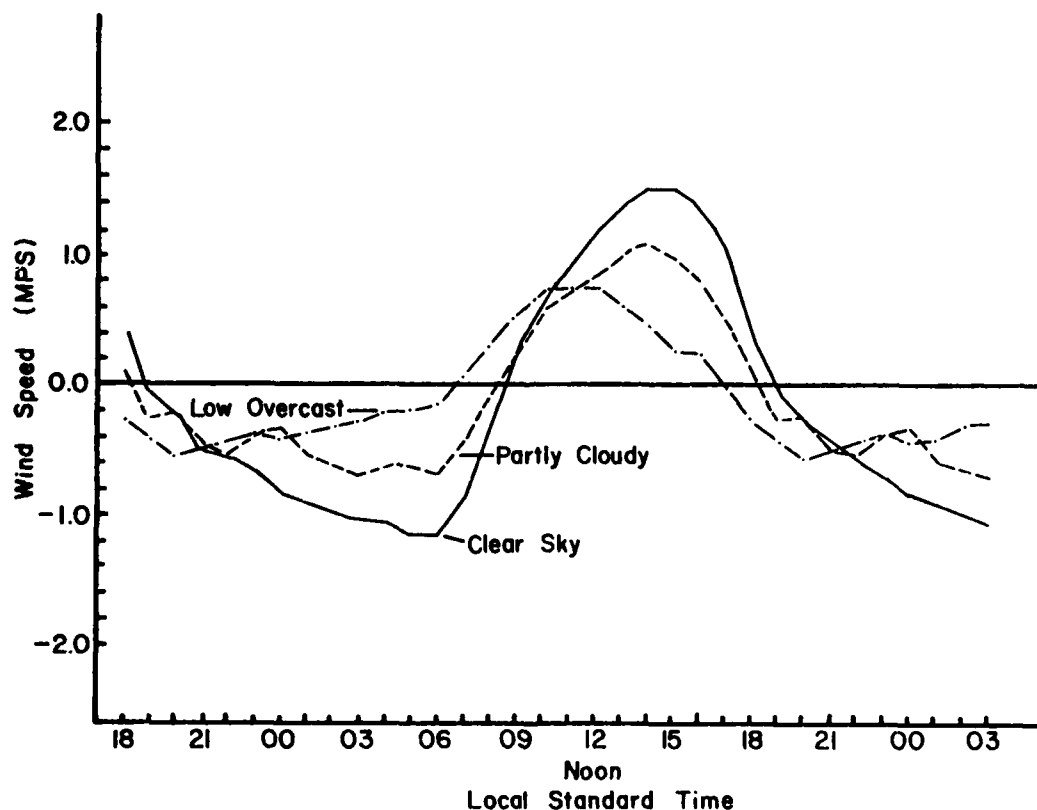


Figure 4. Mean Wind Speed Departure vs Time of Day, 3 Cloud Conditions, March

on diurnal wind speed cycle was the cloud cover, defined above. With the wind speed S given in tenths of knots, the derived algorithm is

$$\tilde{S} - S - \bar{S} = (43. - \bar{C}) * f(t)$$

In Figure 4, the diurnal curve for wind speed with clear sky is very similar to that of temperature, implying a common $f(t)$. However, for large cloud amounts, there appears to be a phase shift in the peak wind speed. In this experiment, this phase shift was ignored because the errors that would be incurred would be relatively small and the programming would be considerably simpler.

The March 1983 data were used to develop the following algorithm for temperature, where T is expressed in tenths of degrees Celsius:

$$\tilde{T} = T - \bar{T} = (5000 - 116 * \bar{C}) * f(t) / (1 + 7.3 * \sqrt{\tilde{S}})$$

(Values of \tilde{S} less than 10 or 1 knot are made equal to 10.)

Next the values for the diurnal $\tilde{V} = 10 * \ln V$ are approximated by

$$\tilde{V} = V - \bar{V} = (31. - .046 * \bar{V}) * \tilde{T} / 75$$

If V and not \tilde{V} is known, the equation can still be easily solved. This formulation is probably an oversimplification, and, since there were few very low visibilities in the data base, one should not expect good performance with dense fog.

Difficulties were encountered in trying to find obvious diurnal patterns in wind direction. Averaged over all stations, there was some tendency for a counter-clockwise shift of a few degrees in the evening and a clockwise shift in mid-morning. However, the amplitudes were of the order of 4 degrees for strong winds and 10 degrees for weak winds. Such small values would have little effect on the vector wind changes from hour to hour. Undoubtedly, at some individual stations, there are much larger systematic wind direction diurnal patterns associated with local terrain, but the advection forecast equations would be difficult to solve without a universal expression. Thus, the diurnal amplitude used for wind direction A was $\tilde{A} = A - \bar{A} = 0$.

Similarly, there were also difficulties finding consistent diurnal dewpoint temperature patterns. Again, local effects may be important, and, in addition, a variety of sensor problems may be involved. A more pronounced dewpoint diurnal cycle would probably be seen in the summer, but, for this March experiment, we assumed for dewpoint H that $\tilde{H} = H - \bar{H} = 0$.

A careful look at the shapes of the diurnal curves reveals obvious problems to fitting simple sine or cosine functions. Physically, it is possible that the combina-

tion of rising sun, changing boundary layer depth, and outgoing radiation could produce an approximate sinusoidal pattern from dawn to late afternoon. However, by sunset, the process changes to one of net outgoing radiation that decreases in magnitude as the temperature falls, more like an exponential decay process. For this reason, essentially two algorithms were constructed, one for day and one for night. In the following expressions, t represents the time in hours past 0600 local sun time.

$$0615 \text{ to } 1715 \text{ LST } f(t) = .60 * \cos \left[(t - 9.0) \frac{\pi}{12} \right] - .06$$

$$1715 \text{ to } 0615 \text{ LST } f(t) = .98 * \exp [- .2 * (t - 11.5)] - .564$$

Besides inclusion of the diurnal change expressions in the forecast equations and the addition of the 700-500 mb space-smoothed steering field (700-500S), one more change was made in the forecast procedure. One problem perceived in the forecasting of surface wind was the presence of high frequency fluctuations in the nominal 1-minute averaged wind transmitted every hour.¹⁴ These fluctuations are caused by boundary layer turbulence and would probably introduce noise into the analyses and errors into the forecasts. Unfortunately, the data in the hourly reports are not sufficient to properly filter out the turbulent contribution. An attempt was made in this direction by time averaging the u and v grid fields with those of the hour before. The latest and prior observations should also have been averaged for use in the change-advection routine, but this step was neglected in the forecast program.

The data processing consisted of generating some 26 analysis grids on the AFGL McIDAS for each of the 12 cases and placing the grids on tape. On a case-by-case basis, forecasts were generated and verified on the AFGL computer (with the scores saved on disk files). After all cases were processed, scores for the complete experiment were computed. Having scores for individual cases allowed for a later check into systematic differences for different overall weather conditions. The resulting skill scores are presented in Tables 3a, 3b, 3c, 3d, 3e, and 3f. The rms forecast errors are shown graphically in Figures 5a, 5b, 5c, 5d, 5e, and 5f for persistence and the 700-500S advection and change-advection forecasts as well as the NMC-MOS forecasts. Figures 6a, 6b, 6c, 6d, and 6e illustrate the effects of adding the diurnal algorithms to the forecast routines by examining the mean-arithmetic error, or bias.

Overall, the results of Experiment III are quite similar to Experiments I and II. The advection forecasts for vector wind show positive skill beginning about 2-

15. Muench, H.S. (1982) An Appraisal of the Short-Range Forecast Problem Using Power Spectra, AFGL-TR-82-0353, AD A129315.

Table 3a. Advection Forecast Experiment III, Skill Scores Relative to Persistence, Vector Wind

TECHNIQUE/TIME (H)	VECTOR WIND (rms error, mps, in parentheses)														
	0	1	2	3	4	6	9	12	15						
Persistence	(±0.00)	(±2.12)	(±2.90)	(±3.07)	(±3.61)	(±4.04)	(4.82)	(±6.01)	(±6.34)						
Persistence + Diurn.	(±0.00)	+0.00	-0.01	-0.02	-0.04	-0.03	+0.00	+0.01	+0.00						
Advection 700 mb	(±1.81)	-0.06	+0.00	+0.07	+0.10	+0.12	+0.16	+0.22	+0.22						
Advection 7-5F	(±1.81)	-0.04	+0.02	+0.10	+0.14	+0.14	+0.20	+0.25	+0.26						
Advection 7-5S	(±1.81)	-0.05	+0.00	+0.09	+0.14	+0.15	+0.22	+0.28	+0.28						
Adv. + Diurn. 700 mb	(±1.81)	-0.07	-0.01	+0.07	+0.11	+0.03	+0.16	+0.23	+0.20						
Adv. + Diurn. 7-5F	(±1.81)	-0.05	+0.02	+0.11	+0.15	+0.15	+0.20	+0.25	+0.26						
Adv. + Diurn. 7-5S	(±1.81)	-0.06	+0.00	+0.09	+0.14	+0.16	+0.22	+0.28	+0.27						
Chng Adv. 700 mb	(±0.00)	-0.01	-0.01	-0.01	+0.02	+0.00	-0.08	-0.10	-0.14						
Chng Adv. 7-5F	(±0.00)	-0.01	-0.01	+0.00	+0.03	-0.01	-0.09	-0.11	-0.18						
Chng Adv. 7-5S	(±0.00)	+0.00	+0.00	+0.02	+0.07	+0.01	-0.05	-0.08	-0.14						
Chng Adv. + Diurn. 700 mb	(±0.00)	-0.01	-0.03	-0.06	-0.03	-0.01	-0.07	-0.06	-0.12						
Chng Adv. + Diurn. 7-5F	(±0.00)	-0.01	-0.03	-0.06	-0.02	-0.07	-0.07	-0.05	-0.14						
Chng Adv. + Diurn. 7-5S	(±0.00)	-0.01	-0.01	-0.03	-0.01	-0.03	-0.03	-0.01	-0.10						
NMC-MOS	(±0.00)	xxx	xxx	+0.01	xxx	xxx	+0.30	xxx	+0.42						

tion of rising sun, changing boundary layer depth, and outgoing radiation could produce an approximate sinusoidal pattern from dawn to late afternoon. However, by sunset, the process changes to one of net outgoing radiation that decreases in magnitude as the temperature falls, more like an exponential decay process. For this reason, essentially two algorithms were constructed, one for day and one for night. In the following expressions, t represents the time in hours past 0600 local sun time.

$$0615 \text{ to } 1715 \text{ LST } f(t) = .60 * \cos \left[(t - 9.0) \frac{\pi}{12} \right] - .06$$

$$1715 \text{ to } 0615 \text{ LST } f(t) = .98 * \exp [-.2 * (t - 11.5)] - .564$$

Besides inclusion of the diurnal change expressions in the forecast equations and the addition of the 700-500 mb space-smoothed steering field (700-500S), one more change was made in the forecast procedure. One problem perceived in the forecasting of surface wind was the presence of high frequency fluctuations in the nominal 1-minute averaged wind transmitted every hour.¹⁴ These fluctuations are caused by boundary layer turbulence and would probably introduce noise into the analyses and errors into the forecasts. Unfortunately, the data in the hourly reports are not sufficient to properly filter out the turbulent contribution. An attempt was made in this direction by time averaging the u and v grid fields with those of the hour before. The latest and prior observations should also have been averaged for use in the change-advection routine, but this step was neglected in the forecast program.

The data processing consisted of generating some 26 analysis grids on the AFGL McIDAS for each of the 12 cases and placing the grids on tape. On a case-by-case basis, forecasts were generated and verified on the AFGL computer (with the scores saved on disk files). After all cases were processed, scores for the complete experiment were computed. Having scores for individual cases allowed for a later check into systematic differences for different overall weather conditions. The resulting skill scores are presented in Tables 3a, 3b, 3c, 3d, 3e, and 3f. The rms forecast errors are shown graphically in Figures 5a, 5b, 5c, 5d, 5e, and 5f for persistence and the 700-500S advection and change-advection forecasts as well as the NMC-MOS forecasts. Figures 6a, 6b, 6c, 6d, and 6e illustrate the effects of adding the diurnal algorithms to the forecast routines by examining the mean-arithmetic error, or bias.

Overall, the results of Experiment III are quite similar to Experiments I and II. The advection forecasts for vector wind show positive skill beginning about 2-

15. Muench, H.S. (1982) An Appraisal of the Short-Range Forecast Problem Using Power Spectra, AFGL-TR-82-0353, AD A129315.

Table 3b. Advection Forecast Experiment III, Skill Scores Relative to Persistence, Wind Speed

TECHNIQUE/TIME (H)	WIND SPEED (rms error, mps, in parentheses)														
	0	1	2	3	4	6	9	12	15						
Persistence	(±0.00)	(±1.13)	(±1.46)	(±1.63)	(±1.90)	(±1.96)	(±2.50)	(±2.74)	(±3.03)						
Persistence + Diurn.	(0.00)	+0.01	+0.00	+0.00	-0.03	-0.03	-0.06	+0.03	+0.11						
Advection 700 mb	(±1.27)	-0.30	-0.31	-0.23	-0.17	-0.14	+0.08	+0.07	+0.14						
Advection 7-5F	(±1.27)	-0.27	-0.28	-0.20	-0.15	-0.17	+0.05	+0.08	+0.06						
Advection 7-5S	(±1.27)	-0.31	-0.36	-0.18	-0.12	-0.12	+0.12	+0.13	+0.12						
Adv. + Diurn. 700 mb	(±1.27)	-0.33	-0.27	-0.15	-0.11	-0.08	+0.04	+0.07	+0.22						
Adv. + Diurn. 7-5F	(±1.27)	-0.29	-0.24	-0.11	-0.07	-0.11	+0.02	+0.07	+0.14						
Adv. + Diurn. 7-5S	(±0.00)	-0.32	-0.31	-0.10	-0.07	-0.01	+0.06	+0.11	+0.17						
Chng Adv. 700 mb	(±0.00)	-0.09	-0.11	-0.09	-0.12	-0.32	-0.60	-0.65	-0.65						
Chng Adv. 7-5F	(±0.00)	-0.09	-0.10	-0.08	-0.10	-0.30	-0.63	-0.66	-0.73						
Chng Adv. 7-5S	(±0.00)	-0.08	-0.10	-0.06	-0.11	-0.25	-0.62	-0.65	-0.71						
Chng Adv. + Diurn. 700 mb	(±0.00)	-0.08	-0.14	-0.14	-0.15	-0.37	-0.52	-0.46	-0.54						
Chng Adv. + Diurn. 7-5F	(±0.00)	-0.08	-0.14	-0.13	-0.14	-0.38	-0.57	-0.50	-0.57						
Chng Adv. + Diurn. 7-5S	(±0.00)	-0.07	-0.13	-0.10	-0.13	-0.33	-0.57	-0.53	-0.59						
NMC-MOS	(±0.00)	xxx	xxx	+0.02	xxx	xxx	+0.21	xxx	+0.30						

Table 3c. Advection Forecast Experiment III, Skill Scores Relative to Persistence, Cloud Cover

TECHNIQUE/TIME (H)	TOTAL CLOUD COVER (rms category error, 0-3)														
	0	1	2	3	4	6	9	12	15						
Persistence	(±0.00)	(±0.44)	(±0.59)	(±0.65)	(±0.72)	(±0.81)	(±1.05)	(±1.21)	(±1.20)						
Persistence + Diurn.	(±0.00)	-0.05	-0.02	+0.00	-0.01	-0.01	+0.00	+0.01	+0.02						
Advection 700 mb	(±0.77)	-0.66	-0.34	-0.28	-0.18	-0.15	-0.05	-0.05	-0.20						
Advection 7-5F	(±0.77)	-0.66	-0.29	-0.23	-0.11	-0.06	+0.03	+0.00	-0.21						
Advection 7-5S	(±0.77)	-0.68	-0.31	-0.18	+0.01	+0.00	-0.06	-0.13	-0.36						
Adv. + Diurn. 700mb	(±0.77)	-0.59	-0.31	-0.22	-0.15	-0.11	-0.04	-0.07	-0.23						
Adv. + Diurn. 7-5F	(±0.77)	-0.59	-0.25	-0.17	-0.08	-0.06	+0.02	-0.02	-0.24						
Adv. + Diurn. 7-5S	(±0.77)	-0.61	-0.25	-0.14	+0.06	+0.00	-0.02	-0.15	-0.40						
Chng Adv. 700mb	(±0.00)	-0.02	-0.15	-0.20	-0.26	-0.28	-0.42	-0.69	-1.21						
Chng Adv. 7-5F	(±0.00)	-0.02	-0.15	-0.20	-0.26	-0.31	-0.47	-0.80	-1.23						
Chng Adv. 7-5S	(±0.00)	-0.02	-0.12	-0.14	-0.22	-0.25	-0.43	-0.83	-1.23						
Chng Adv. + Diurn. 700mb	(±0.00)	-0.05	-0.17	-0.23	-0.28	-0.27	-0.36	-0.65	-1.23						
Chng Adv. + Diurn. 7-5F	(±0.00)	-0.05	-0.17	-0.23	-0.28	-0.31	-0.43	-0.89	-1.23						
Chng Adv. + Diurn. 7-5S	(±0.00)	-0.07	-0.14	-0.14	-0.22	-0.22	-0.41	-0.89	-1.24						
NMC-MOS	(±0.00)	xxx	xxx	-0.28	xxx	xxx	+0.28	xxx	+0.28						

Table 3b. Advection Forecast Experiment III, Skill Scores Relative to Persistence, Wind Speed

TECHNIQUE/TIME (H)	WIND SPEED (rms error, mps, in parentheses)														
	0	1	2	3	4	6	8	12	15						
Persistence	(±0.00)	(±1.13)	(±1.46)	(±1.63)	(±1.90)	(±1.96)	(±2.50)	(±2.74)	(±3.03)						
Persistence + Diurn.	(0.00)	+0.01	+0.00	+0.00	-0.03	-0.03	-0.06	+0.03	+0.11						
Advection 700 mb	(±1.27)	-0.30	-0.31	-0.23	-0.17	-0.14	+0.08	+0.07	+0.14						
Advection 7-5F	(±1.27)	-0.27	-0.28	-0.20	-0.15	-0.17	+0.05	+0.08	+0.06						
Advection 7-5S	(±1.27)	-0.31	-0.36	-0.18	-0.12	-0.12	+0.12	+0.13	+0.12						
Adv. + Diurn. 700 mb	(±1.27)	-0.33	-0.27	-0.15	-0.11	-0.08	+0.04	+0.07	+0.22						
Adv. + Diurn. 7-5F	(±1.27)	-0.29	-0.24	-0.11	-0.07	-0.11	+0.02	+0.07	+0.14						
Adv. + Diurn. 7-5S	(±0.00)	-0.32	-0.31	-0.10	-0.07	-0.01	+0.06	+0.11	+0.17						
Chng Adv. 700 mb	(±0.00)	-0.09	-0.11	-0.09	-0.12	-0.32	-0.60	-0.65	-0.65						
Chng Adv. 7-5F	(±0.00)	-0.09	-0.10	-0.08	-0.10	-0.30	-0.63	-0.66	-0.73						
Chng Adv. 7-5S	(±0.00)	-0.08	-0.10	-0.06	-0.11	-0.25	-0.62	-0.65	-0.71						
Chng Adv. + Diurn. 700 mb	(±0.00)	-0.08	-0.14	-0.14	-0.15	-0.37	-0.52	-0.46	-0.54						
Chng Adv. + Diurn. 7-5F	(±0.00)	-0.08	-0.14	-0.13	-0.14	-0.38	-0.57	-0.50	-0.57						
Chng Adv. + Diurn. 7-5S	(±0.00)	-0.07	-0.13	-0.10	-0.13	-0.33	-0.57	-0.53	-0.59						
NMC-MOS	(±0.00)	xxx	xxx	+0.02	xxx	xxx	+0.21	xxx	+0.30						

Table 3d. Advection Forecast Experiment III, Skill Scores Relative to Persistence, Visibility

TECHNIQUE/TIME (H)	LN VISIBILITY (rms error in parentheses)														
	0	1	2	3	4	6	9	12	15						
Persistence	(±0.00)	(±0.35)	(±0.44)	(±0.54)	(±0.64)	(±0.73)	(±0.89)	(±0.93)	(±1.04)						
Persistence + Diurn.	(±0.00)	+0.00	+0.05	+0.07	+0.06	+0.07	+0.04	-0.03	-0.11						
Advection 700 mb	(±0.39)	-0.29	-0.05	+0.04	+0.11	+0.12	+0.07	+0.05	+0.13						
Advection 7-5F	(±0.39)	-0.23	+0.02	+0.07	+0.17	+0.14	+0.11	+0.17	+0.16						
Advection 7-5S	(±0.39)	-0.23	-0.07	+0.04	+0.19	+0.12	+0.08	+0.24	+0.21						
Adv. + Diurn. 700 mb	(±0.39)	-0.60	-0.09	+0.06	+0.16	+0.18	+0.18	+0.22	+0.02						
Adv. + Diurn. 7-5F	(±0.39)	-0.49	-0.02	+0.07	+0.16	+0.18	+0.20	+0.22	+0.04						
Adv. + Diurn. 7-5S	(±0.39)	-0.54	-0.09	+0.00	+0.14	+0.16	+0.19	+0.23	-0.04						
Chng Adv. 700 mb	(±0.00)	+0.03	-0.02	-0.06	-0.06	-0.11	-0.12	-0.39	-0.40						
Chng Adv. 7-5F	(±0.00)	+0.03	-0.07	-0.07	-0.06	-0.15	-0.11	-0.40	-0.47						
Chng Adv. 7-5S	(±0.00)	+0.00	-0.02	-0.02	-0.02	-0.11	-0.11	-0.19	-0.38						
Chng Adv. + Diurn. 700 mb	(±0.00)	-0.03	-0.05	-0.07	-0.14	-0.33	-0.60	-1.11	-1.70						
Chng Adv. + Diurn. 7-5F	(±0.00)	-0.03	-0.05	-0.09	-0.13	-0.34	-0.57	-1.06	-1.51						
Chng Adv. + Diurn. 7-5S	(±0.00)	+0.00	-0.02	-0.07	-0.08	-0.36	-0.74	-1.26	-2.06						
NMC-MOS	(±0.00)	xxx	xxx	-0.28	xxx	xxx	+0.10	xxx	+0.37						

Table 3e. Advection Forecast Experiment III, Skill Scores Relative to Persistence, Temperature

TECHNIQUE/TIME (H)	TEMPERATURE (rms error, Celsius, in parentheses)														
	0	1	2	3	4	6	9	12	15						
Persistence	(±0.00)	(±1.38)	(±2.01)	(±2.70)	(±3.01)	(±3.59)	(±3.03)	(±3.19)	(±4.47)						
Persistence + Diurn.	(±0.00)	+0.17	+0.27	+0.25	+0.24	+0.21	+0.13	+0.06	+0.14						
Advection 700 mb	(±0.85)	-0.41	-0.40	-0.35	-0.29	-0.25	-0.41	-0.49	-0.37						
Advection 7-5F	(±0.85)	-0.36	-0.29	-0.28	-0.22	-0.22	-0.26	-0.24	-0.21						
Advection 7-5S	(±0.85)	-0.36	-0.41	-0.36	-0.29	-0.25	-0.37	-0.31	-0.27						
Adv. + Diurn. 700 mb	(±0.85)	-0.32	-0.17	-0.10	+0.00	+0.03	-0.22	-0.55	-0.47						
Adv. + Diurn. 7-5F	(±0.85)	-0.28	-0.05	-0.01	+0.06	+0.06	-0.09	-0.26	-0.26						
Adv. + Diurn. 7-5S	(±0.85)	-0.29	-0.17	-0.13	-0.02	+0.02	-0.20	-0.35	-0.37						
Chng Adv. 700 mb	(±0.00)	+0.28	+0.35	+0.39	+0.28	+0.08	-1.15	-2.69	-2.48						
Chng Adv. 7-5F	(±0.00)	+0.28	+0.35	+0.39	+0.28	+0.09	-1.11	-2.61	-2.46						
Chng Adv. 7-5S	(±0.00)	+0.28	+0.35	+0.40	+0.31	+0.11	-1.08	-2.58	-2.48						
Chng Adv. + Diurn. 700 mb	(±0.00)	+0.28	+0.31	+0.34	+0.29	+0.27	-0.02	-0.43	-0.33						
Chng Adv. + Diurn. 7-5F	(±0.00)	+0.28	+0.30	+0.36	+0.30	+0.26	+0.00	-0.42	-0.36						
Chng Adv. + Diurn. 7-5S	(±0.00)	+0.28	+0.31	+0.34	+0.32	+0.24	-0.07	-0.48	-0.31						
NMC-MOS	(±0.00)	xxx	xxx	+0.36	xxx	+0.50	+0.46	+0.38	+0.38						

Table 3f. Advection Forecast Experiment III, Skill Scores Relative to Persistence, Dewpoint

TECHNIQUE/TIME (H)	DEWPOINT TEMPERATURE (rms error, Celsius, in parentheses)														
	0	1	2	3	4	6	9	12	15						
Persistence	(±0.00)	(±1.08)	(±1.57)	(±1.78)	(±2.01)	(±2.36)	(±3.21)	(±4.07)	(±4.89)						
Persistence + Diurn.	(±0.00)	xxx	xxx	xxx	xxx	xxx	xxx	xxx	xxx						
Advection 700 mb	(±1.12)	-0.31	-0.07	-0.01	-0.01	-0.16	-0.11	-0.11	-0.07						
Advection 7-5F	(±1.12)	-0.32	+0.00	+0.08	+0.06	-0.05	-0.03	+0.01	-0.01						
Advection 7-5S	(±1.12)	-0.39	-0.02	-0.01	-0.05	-0.01	+0.03	+0.08	+0.08						
Adv. + Diurn. 700 mb	(±1.12)	xxx	xxx	xxx	xxx	xxx	xxx	xxx	xxx						
Adv. + Diurn. 7-5F	(±1.12)	xxx	xxx	xxx	xxx	xxx	xxx	xxx	xxx						
Adv. + Diurn. 7-5S	(±1.12)	xxx	xxx	xxx	xxx	xxx	xxx	xxx	xxx						
Chng Adv. 700 mb	(±0.00)	-0.10	-0.15	-0.14	-0.26	-0.46	-0.52	-0.63	-0.70						
Chng Adv. 7-5F	(±0.00)	-0.11	-0.15	-0.13	-0.25	-0.44	-0.55	-0.60	-0.66						
Chng Adv. 7-5S	(±0.00)	-0.11	-0.13	-0.10	-0.23	-0.36	-0.39	-0.39	-0.42						
Chng Adv. + Diurn. 700 mb	(±0.00)	xxx	xxx	xxx	xxx	xxx	xxx	xxx	xxx						
Chng Adv. + Diurn. 7-5F	(±0.00)	xxx	xxx	xxx	xxx	xxx	xxx	xxx	xxx						
Chng Adv. + Diurn. 7-5S	(±0.00)	xxx	xxx	xxx	xxx	xxx	xxx	xxx	xxx						
NMC-MOS	(±0.00)	xxx	xxx	-0.02	xxx	+0.25	+0.49	+0.44	+0.53						

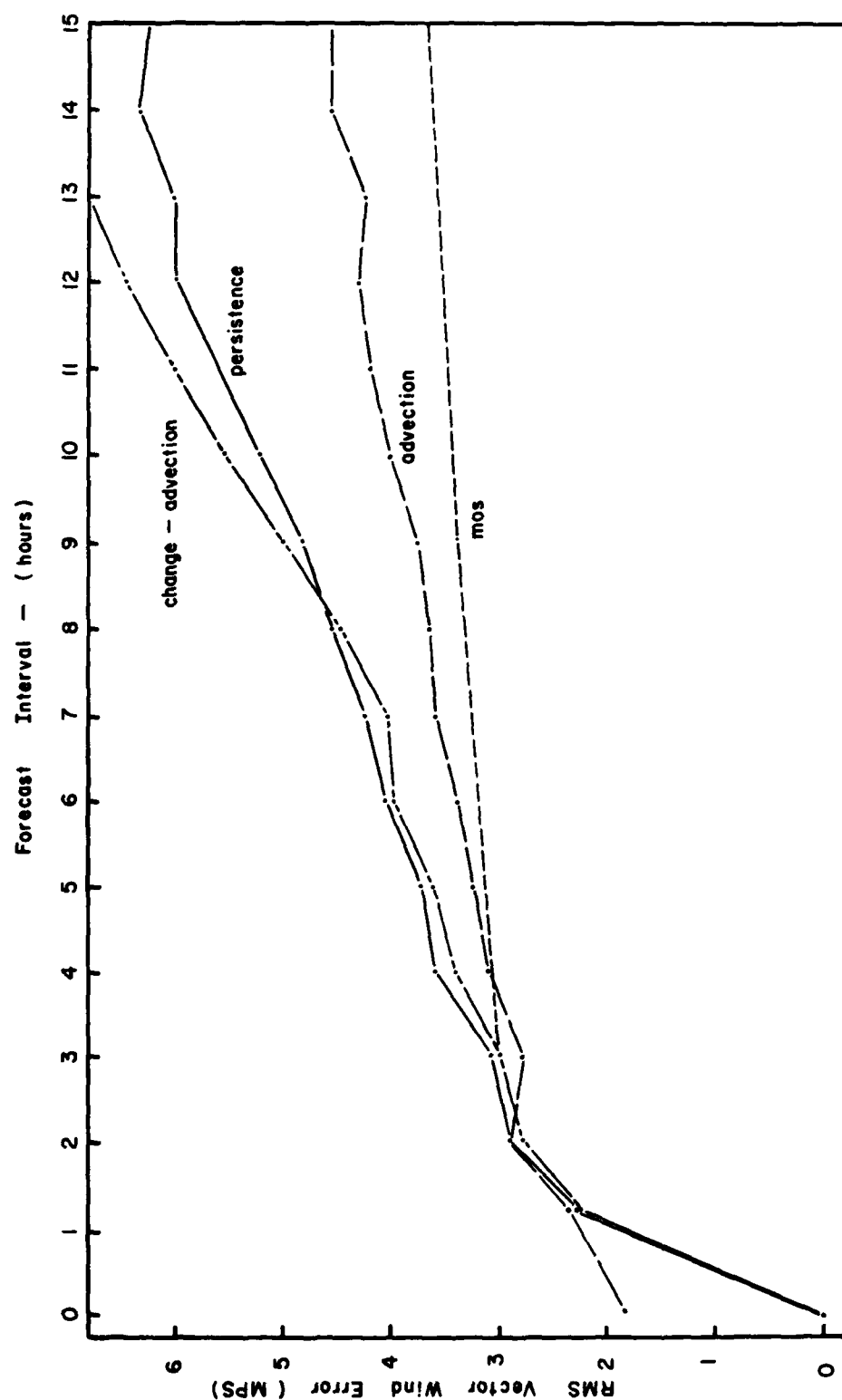


Figure 5a. RMS Wind Vector vs Forecast Time, Advection Forecast Experiment III, 700-500S Flow

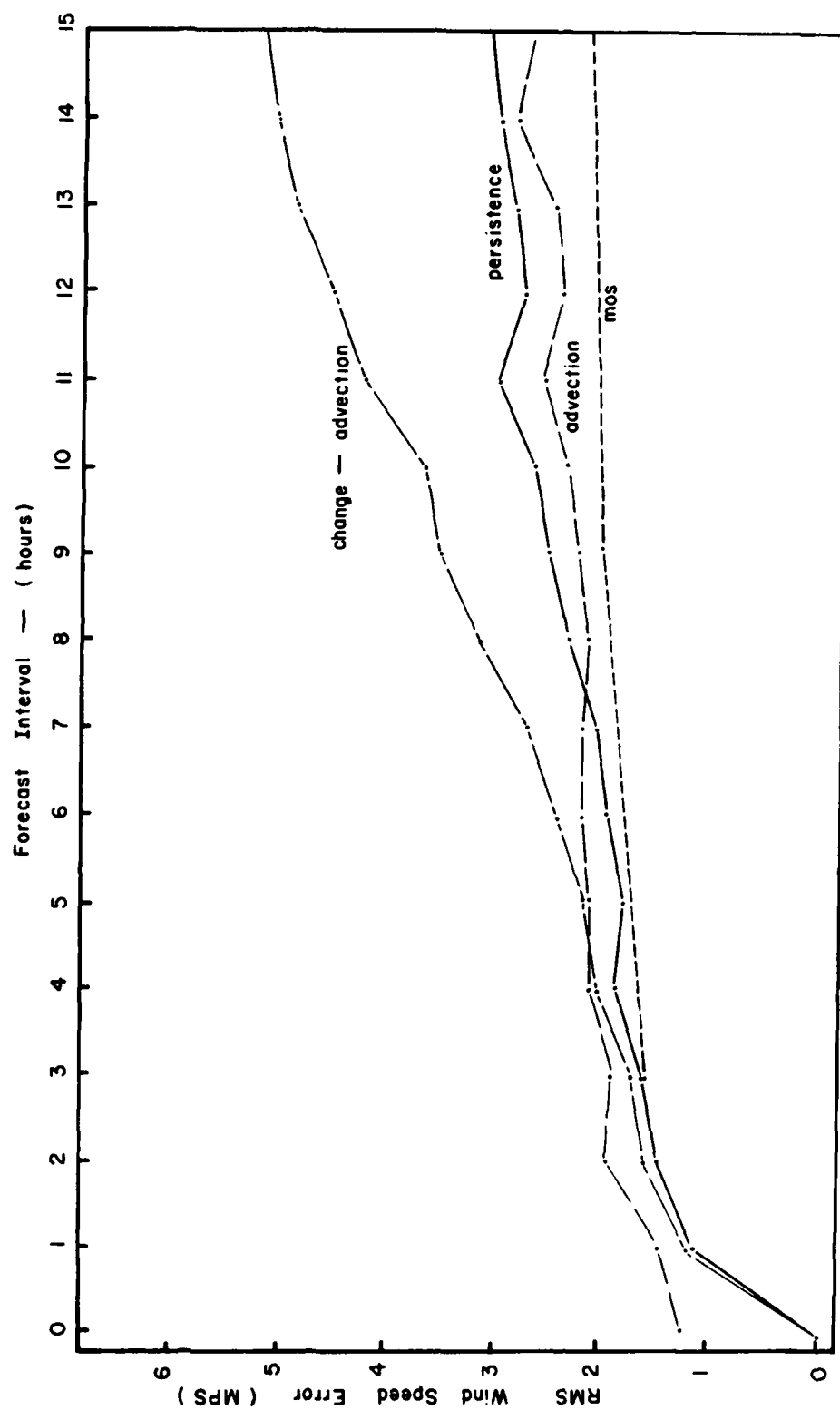


Figure 5b. RMS Wind Speed vs Forecast Time, Advection Forecast Experiment III, 700-500S Flow

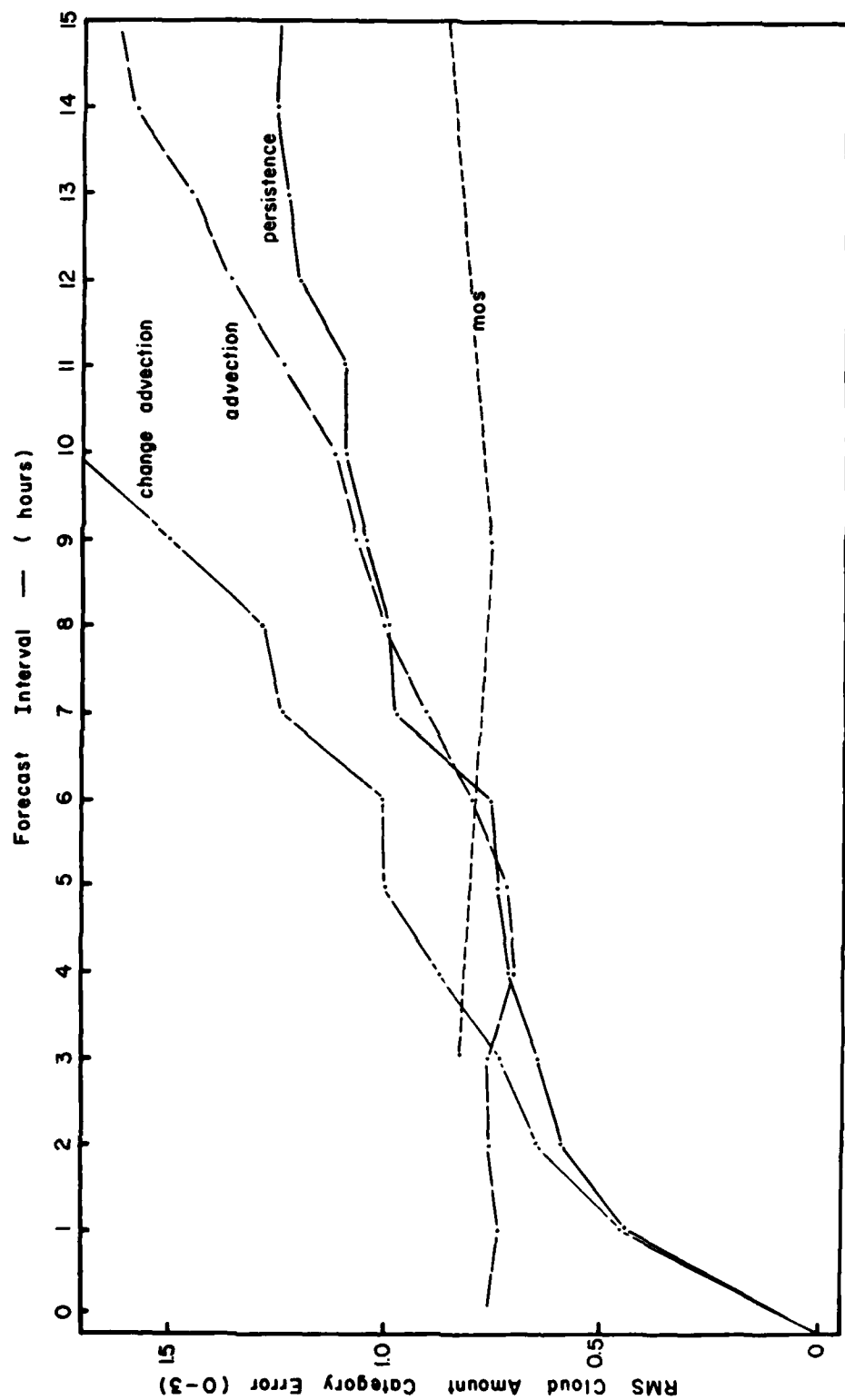


Figure 5c. RMS Cloud Amount vs Forecast Time, Advection Forecast Experiment III, 700-500S Flow

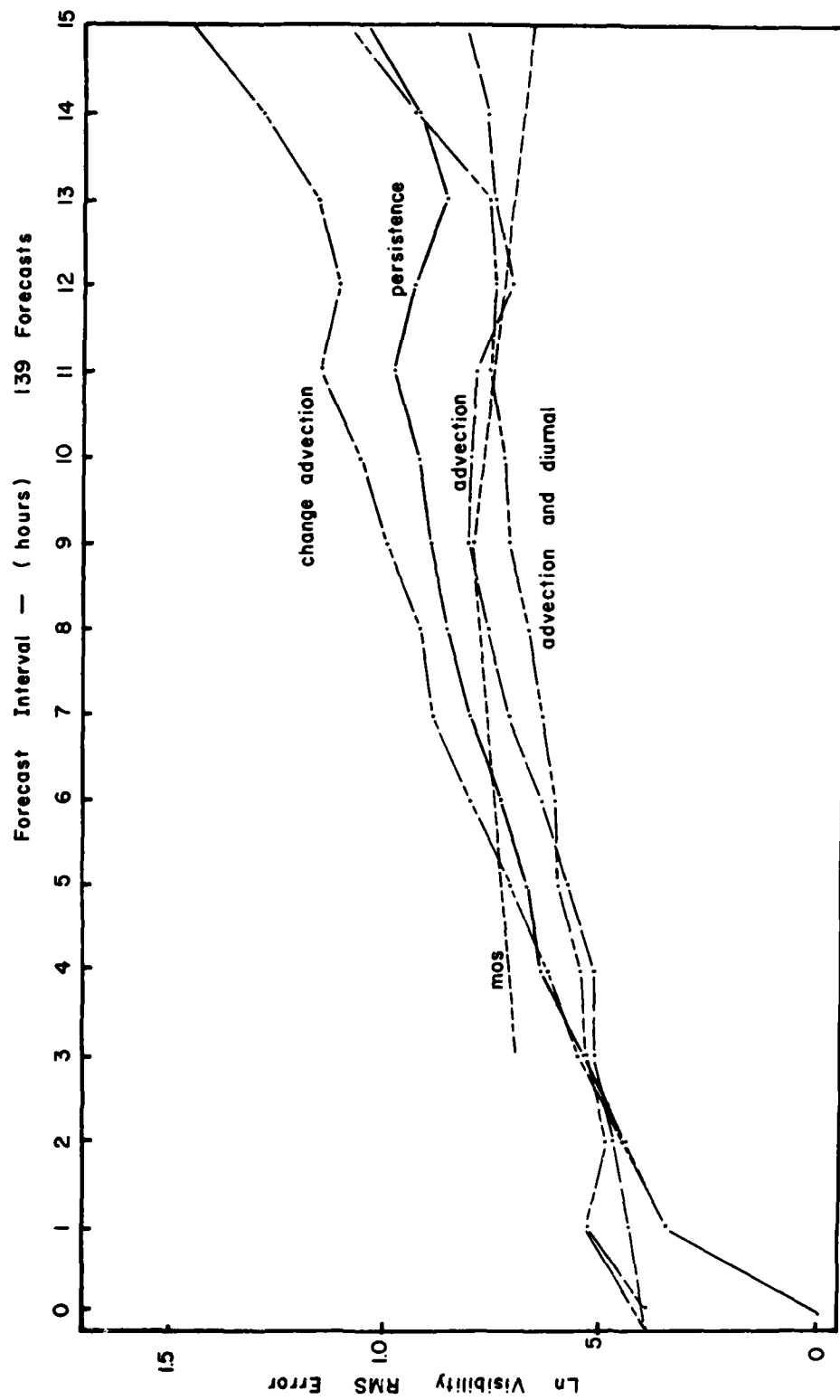


Figure 5d. RMS \ln Visibility vs Forecast Time, Advection Forecast Experiment III, 700-500S Flow

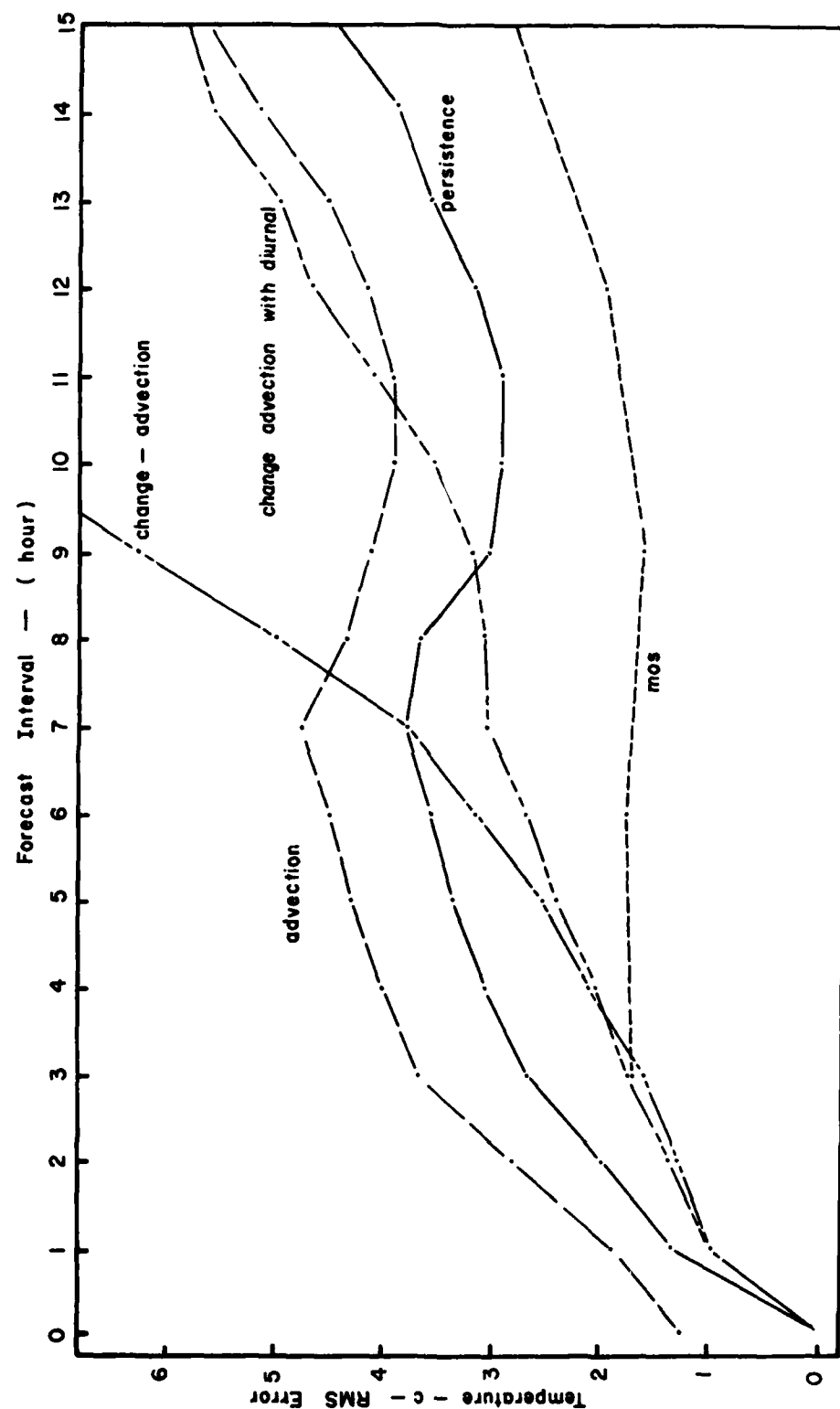


Figure 5e. RMS Temperature vs Forecast Time, Advection Forecast Experiment III, 700-500S Flow

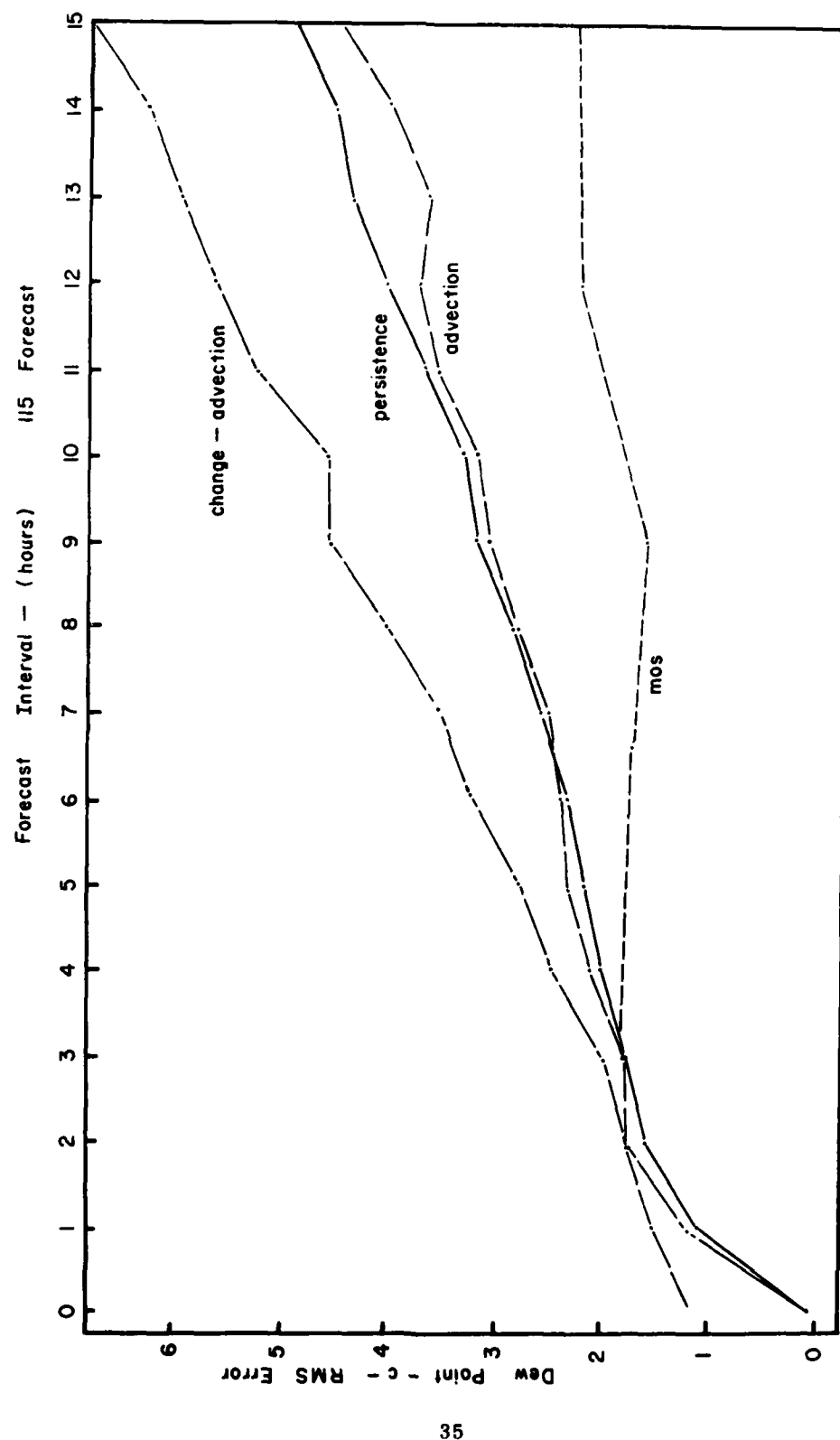


Figure 5f. RMS Dewpoint vs Forecast Time, Advection Forecast Experiment III, 700-500S Flow

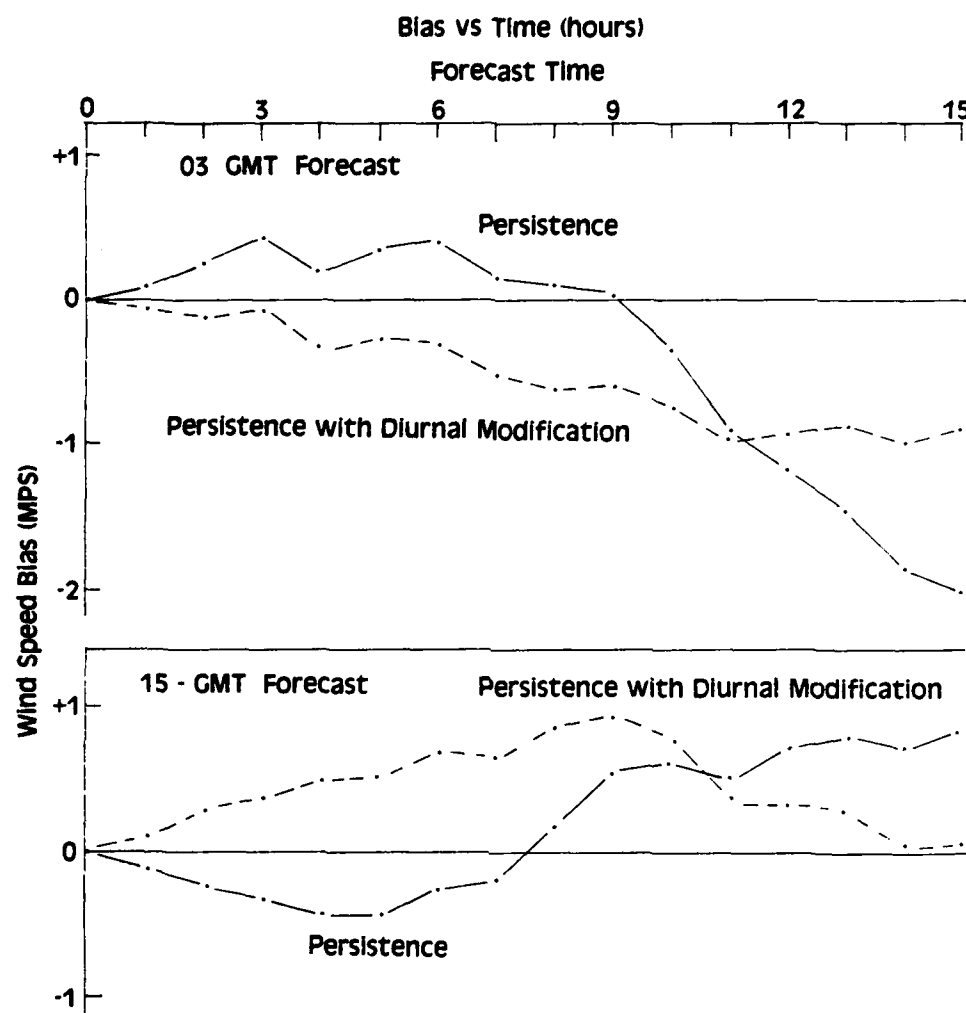


Figure 6a. Persistence Bias vs Forecast Time, Wind Speed, Advection Forecast Experiment III

3 hours. The scores for 1-3 hours, though small, are somewhat better than previous tests. These results may have been caused by the introduction of time-averaged winds (on grids). Had the latest observations also been time-averaged, there would probably have been a similar improvement in the change-advection scores compared to Experiment II. One disappointment in these results is the lack of improvement when the diurnal algorithms were added to the forecast routines. The reason can be inferred from Figure 6a, which shows, in effect, that the addition of the diurnal to persistence overcompensated for the diurnal changes. The resulting

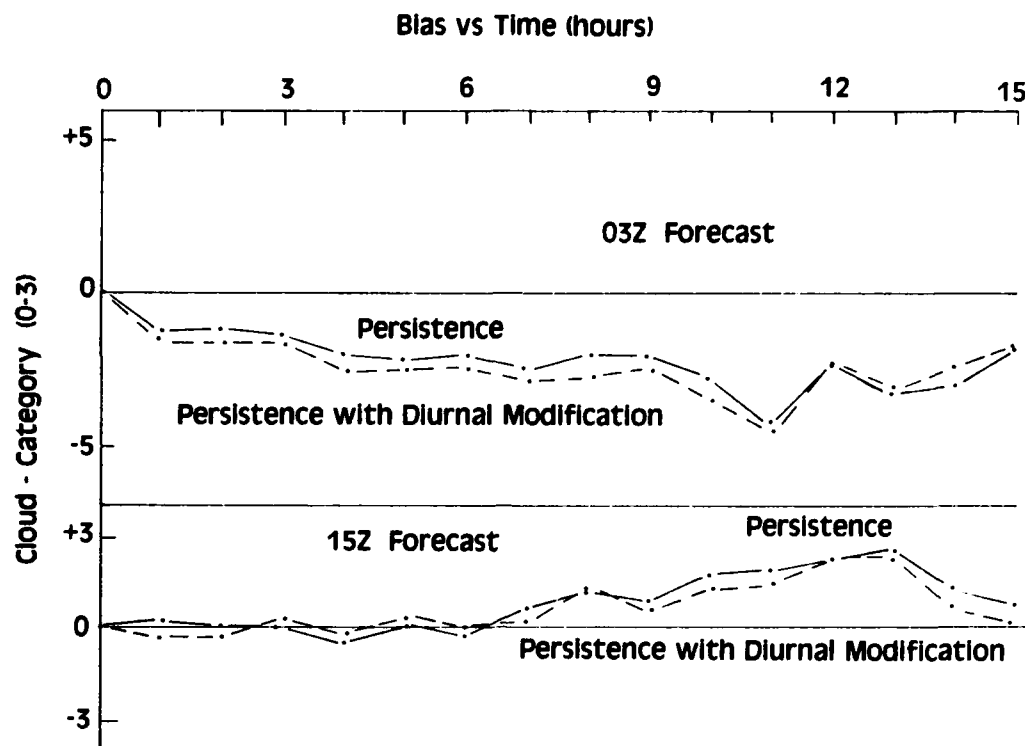


Figure 6b. Persistence Bias vs Forecast Time, Cloud Amount, Advection Forecast Experiment III.

biases were of sign opposite to that of simple persistence for both 03-GMT and 15-GMT forecasts. The overcompensation appears to be the result of an encoding error; the error will be corrected for future tests. However, considering that the diurnal changes in speed 03 GMT (or 15 GMT) for a mixture of clear and cloudy cases would be about ± 0.6 mps, representing a small part of persistence error, even a correct diurnal forecast probably would not have produced more than a few percent increase in the skill scores. (Of course, producing even a few percent increase isn't always easy.)

In Experiments II and III, wind speed itself was not forecast, so the relatively low skill scores in Table 3b are somewhat surprising, if not actually puzzling. For instance, why should the advection scores for 3 hours be positive for the wind vector but negative for the wind speed? The inference is that the wind direction changes are being forecast better than the speed changes are.

The main problem appears to be that the wind speeds observed by airways stations are not as compatible with each other as the wind directions are. First, not

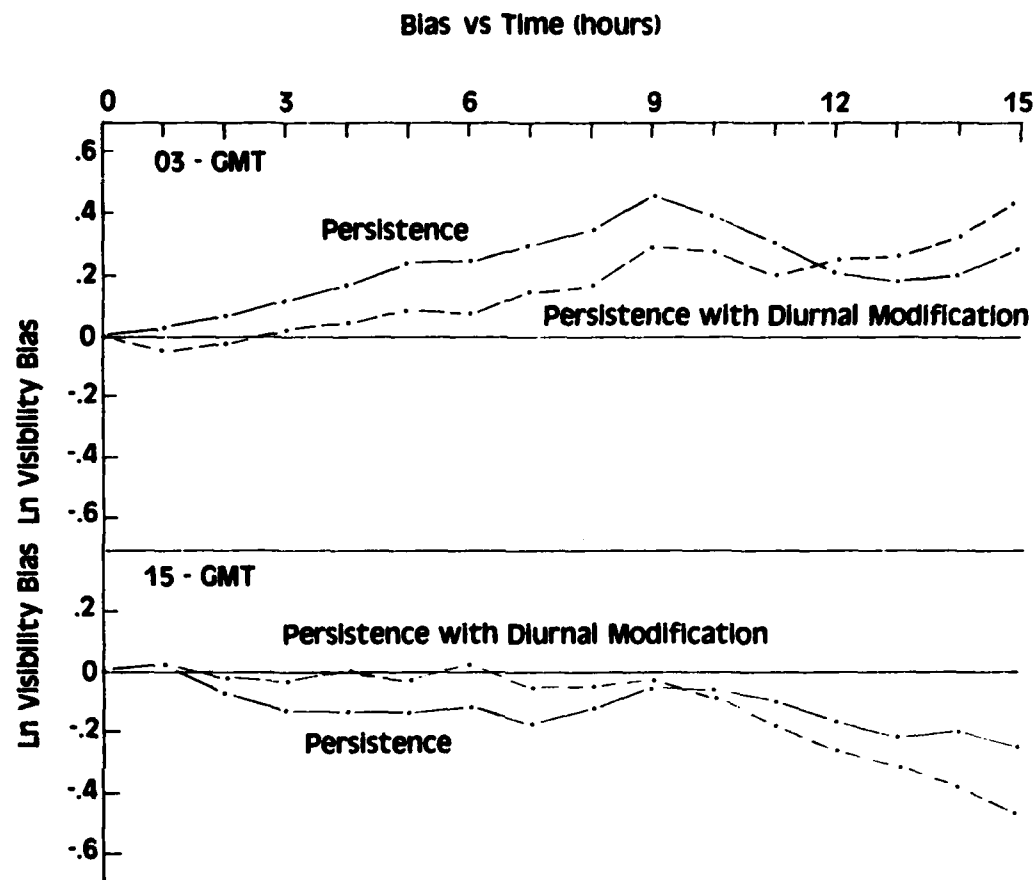


Figure 6c. Persistence Bias vs Forecast Time, Ln Visibility, Advection Forecast Experiment III

all sensors are mounted at the same height above ground. This leads to problems because of the systematic increase in speed with height. A second difficulty, described in some detail by Fujita and Wakimoto,¹⁶ is that the effects of surface roughness and nearby obstructions on wind observations can vary considerably from site to site. To analyze surface wind for making objective forecasts or dynamic computations such as divergence, station-by-station adjustment of wind speed must be made, and, in some cases, the speed adjustments may be direction-dependent. If the wind speed at a given site were systematically slow or fast, at

16. Fujita, T. T., and Wakimoto, R. M. (1982) Effects of miso- and meso-scale obstructions on the PAM winds obtained during project NIMROD, J. of Appl. Meteorol. 21:840-858.

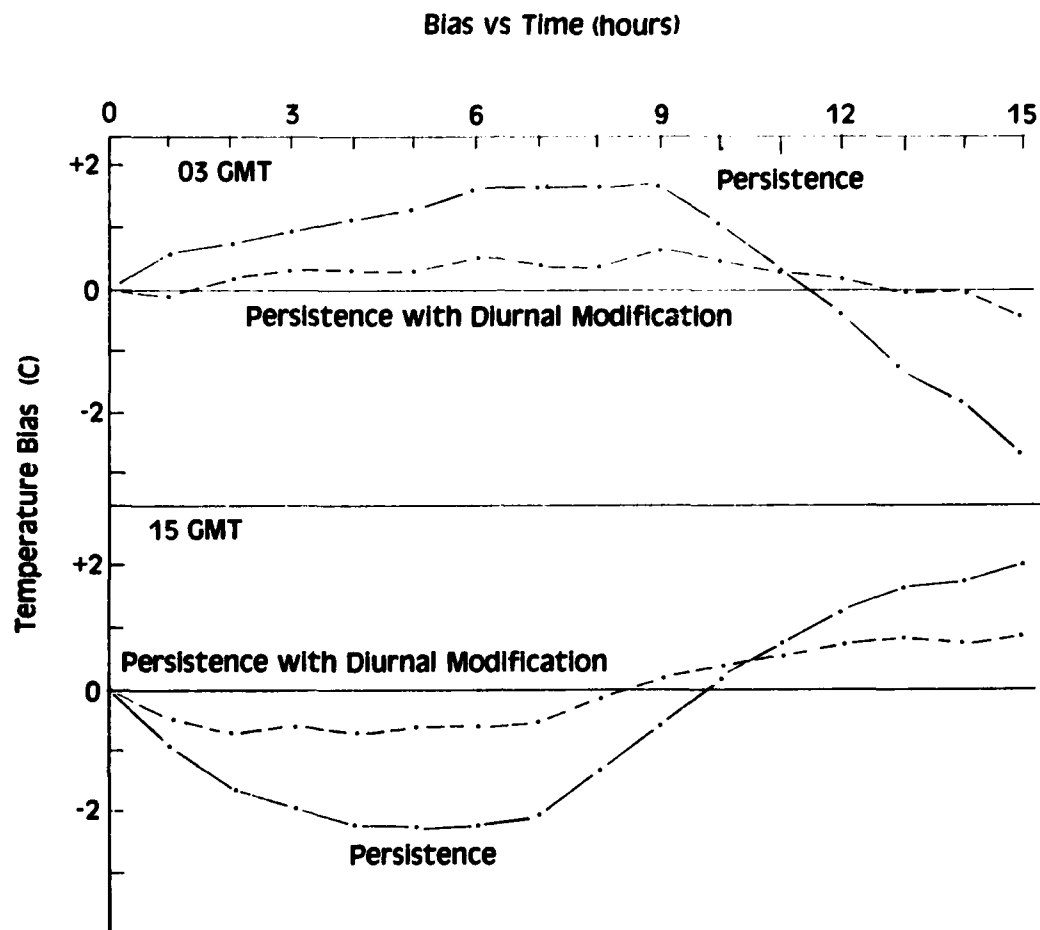


Figure 6d. Persistence Bias vs Forecast Time, Temperature, Advection Forecast Experiment III

least the sign of the changes (though not the magnitude) would be correct. We note in Table 3b that the change-advection scores for wind speed are noticeably better than the scores for advection in the 1-4-hour period, whereas the advection and change-advection scores were similar for the vector winds (Table 3a).

As in previous experiments, the advection skill scores for total cloud amount are low, mostly negative (Table 3c). The diurnal algorithm could probably be improved a little, as both persistence and persistence + diurnal had similar biases as seen in Figure 6c. However, the contributions of the diurnal cycle to overall changes in March are so relatively small, the effort would not be justified. A better way to improve the cloud forecasts would be to use satellite imagery, with

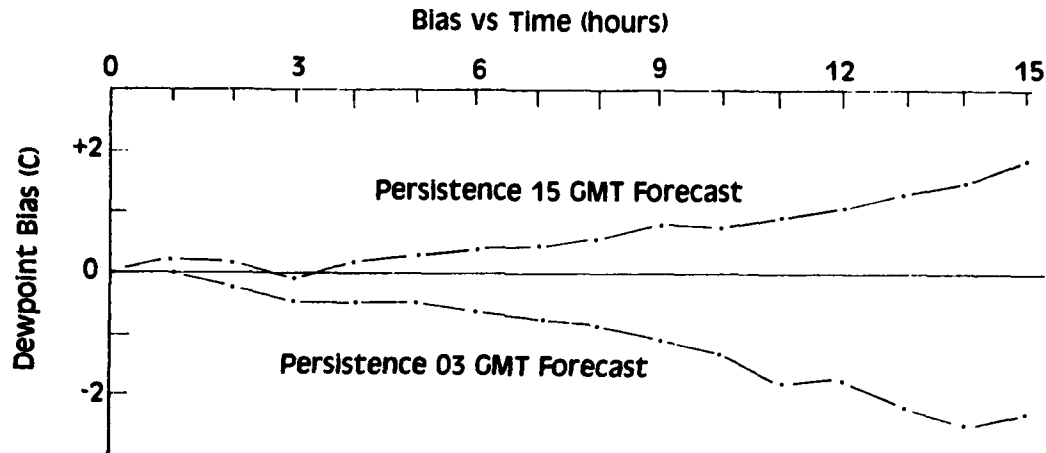


Figure 6e. Persistence Bias vs Forecast Time, Dewpoint, Advection Forecast Experiment III

much higher spatial resolution (and perhaps better consistency), to specify the cloud fields in the advection routines.

The results for the visibility forecasts are encouraging (see Table 3d). The skill scores for advection are positive beyond 2 hours, though the level of skill is *modest*. The diurnal algorithms definitely improve the persistence forecasts out to 9 hours, as indicated by the skill scores in Table 3d and the smaller biases in Figure 6c. During the 12 forecast cases of March 1983, most of the reduced visibility was either directly or indirectly associated with precipitation (mostly rain), so the positive skills may indicate success in advecting precipitation areas, which had been found by Muench⁴ in the satellite-based advection experiments. Low visibility in precipitation cases usually accompanies low cloud-ceiling heights, so there is reason to expect that the advection techniques would also find modest success forecasting ceiling.

As expected, the effects of modifying the forecast techniques for the diurnal change were quite pronounced in the case of temperature. The skill scores for persistence diurnal are themselves high enough to be considered useful. In addition, the bias errors in Figure 6d indicate that further improvement might result from increasing the magnitudes of the diurnal temperature change. The simple advection scores are as poor as those in Experiment II, but the addition of the diurnal cycle improved the scores to the point where there are some positive scores at 4-6 hours out into the forecast. The change-advection scores are again quite good out to 4 hours, but the addition of the diurnal cycle only improved the scores beyond 4 hours. This result is consistent with the earlier suggestion that all the skill for the change-advection in the first 4 hours comes from the extrapolation of

the diurnal: the diurnal modification only subtracted out the diurnal in one place and added it back in another.

The dewpoint forecast skill scores are as low as in Experiment I, and there are obviously some problems. The rms changes for 1-6 hours are somewhat lower than for temperature, so one problem could be that the uncertainties in the measurements are causing changes as large as the real changes (or larger). However, the failure of advection to produce skillful forecasts for either temperature or dewpoint at 12 hours, when changes are larger, raises a question of whether the wrong steering was used. Physically, rather than using 700 mb or 500 mb, the 850- or even 1000-mb level may be more reasonable. In these experiments, the higher levels were used in the belief that they would better portray the combined effects of advection and the modifying effects that clouds and precipitation have on temperature and dewpoint.

5. CONCLUSIONS AND DISCUSSION

The advection techniques tested thus far have not shown the level of skill relative to persistence that one would like to see for an operational forecast tool in routine use. However, for the 2- to 6-hour period, the techniques could provide useful guidance for wind and visibility, especially since the MOS scores are low for these parameters.

When Experiment III was conducted, forecasts were also verified on a case-by-case basis to see if performance was weather dependent. As a simple test, standard deviations were computed about spatial means, for vector wind (uv), cloud cover (C), temperature (T), and dewpoint (H). The standard deviations were correlated to 3-hour persistence error (or change). The values computed for the 12 cases were $r_{uv} = +.60$, $r_C = +.49$, $r_T = -.24$, and $r_H = +.56$.

For wind, cloud cover, and dewpoint, these correlations indicate a dynamic link between gradients and local change (perhaps advection) and imply that a fair portion of the change may be forecastable. In the case of temperature, there was a -0.66 correlation of rms 3-hour change to area, average cloud cover again showing importance of radiation. When the improvements over persistence for advection were compared to the spatial variability, the correlations were $r_{uv} = +0.30$, $r_C = +0.30$, $r_T = -0.47$, and $r_H = +0.16$. These small positive correlations (except temperature) show the advection routine performs better when gradients are large ("active-looking" situations).

Several steps are still to be taken before the validity of the advection concept can really be tested. As a start, the basic airways reports must be edited before being used in objective forecast procedures. In addition, the parameters must be

"normalized" to reduce local effects (particularly important for wind speed). Temperature, visibility, and, to some extent, dewpoint are not conservative for motions up and down terrain, so some transformations should be made, analogous to "potential temperature," before they are used in advection routines. Next, the analysis routine used was probably too crude, and a more sophisticated "Barnes-type" scheme,¹⁰ using multiple passes, should be tried. And, of course, if satellite imagery were introduced into the procedure, it would certainly improve the cloud forecasting.

The situation in short-range forecasting today may well be similar to the status of synoptic-scale forecasting in the early 1950s, when prognostic charts were prepared manually without computer guidance. At that time, there were considerable differences in skill from one forecaster to another, reflecting, to some extent, their relative abilities at separating signal from noise in the basic data. When objective forecast procedures became available, they equalled the performance of the poorer forecasters at first, and, when improved initialization procedures were introduced into the dynamic models, the skill reached that of the best forecasters. (The biggest advantage of the dynamic model is handling a hemisphere at many levels in the time the synoptician forecasts two levels over the United States.) In the mesoscale, for the 1- to 4-hour period, skill scores of about 0.1 to 0.4 seem to be par at present⁴ for routine subjective forecasts, and, as in the 1950s, individual forecasters differ considerably in skill.¹⁷ If the analogy is applicable, all of the suggested improvements just given might only boost the skill scores to the +0.1 to +0.4 range. Unless the future mesoscale dynamic models can diagnose disturbances the forecasters are missing, even these models may only achieve skills relative to persistence of about +0.4 to +0.5, meaning that half the short-period changes will still be missed. However, regular forecasts of half the changes would still be much better than none.

References

1. Fjörtoft, R. (1952) On a numerical method of integrating the barotropic vorticity equation, Tellus 4:179-194.
2. Estoque, M.A. (1957) A graphical integration of a two-level model, J. Atmos. Sci. 14:38-42.
3. Reed, R.J. (1960) On the practical use of graphical prediction methods, Mon. Wea. Rev. 88:209-218.
4. Muench, H.S. (1981) Short-Range Forecasting of Cloudiness and Precipitation Through Extrapolation of GOES Imagery, AFGL-TR-81-0218, AD A108678.
5. Wash, C.H., and Whittaker, T.M. (1980) Subsynoptic analysis and forecasting with an interactive computer system, Bull. Am. Meteorol. Soc. 61:1584-1591.
6. Glahn, H.R., and Lowry, D. (1972) The use of model output statistics (MOS) in objective weather forecasting, J. Appl. Meteorol. 11:1203-1211.
7. Zurndorfer, E.A.; Bocchieri, J.R.; Carter, G.M.; Dallaville, J.P.; Gilhausen, D.B.; Hebenstreit, K.F.; Vercelli, D.J. (1979) Trends in comparative verification scores for guidance and local aviation weather forecasts, Mon. Wea. Rev. 107:799-811.
8. Cressman, G.P. (1959) An operational objective analysis system, Mon. Wea. Rev. 87:367-371.
9. Gerlach, A., ed. (1982) Objective Analysis and Prediction Techniques, AFGL-TR-82-0394, AD A131465.
10. Barnes, S.L. (1964) A technique for maximizing details in numerical weather map analyses, J. Appl. Meteor. 3:396-409.
11. Revised Uniform Summary of Surface Weather Observations, A-F, U.S. Air Force, AWS (by station) (about 500 pages each, available through NTIS).
12. An Aid for Using the Revised Uniform Summary of Surface Weather Observations (RUSSWO's) (1983) USAF TAC/TN-83/001, Scott AFB, IL 62225.

13. Climatography of the United States No. 82-41, Decennial Census of United States Climate: Summary of Hourly Observations 1951-1960 (by station), Superintendent of Documents, U.S. GPO, Washington, D.C.
14. Hourly Data Summaries No. 1-84 (by station), Climatology Division Meteorological Branch, Department of Transport, Canada.
15. Muench, H.S. (1982) An Appraisal of the Short-Range Forecast Problem Using Power Spectra, AFGL-TR-82-0353, AD A129315.
16. Fujita, T.T., and Wakimoto, R.M. (1982) Effects of miso- and meso-scale obstructions on the PAM winds obtained during project NIMROD, J. of Appl. Meteorol. 21:840-858.